ADDIS ABABA SCIENCE AND TECHNOLOGY UNIVERSITY

SYNTHESIS AND CHARACTERIZATION OF CELLULOSE NANOCRYSTALS FROM WATER HYACINTH USING ACID HYDROLYSIS

By

MULUNEH AYALEW BALCHA

A Thesis Submitted as a Partial Fulfilment to the Requirements for the Award of the Degree of Master of Science in Chemical Engineering

(Chemical Process and Product design)

to

DEPARTMENT OF CHEMICAL ENGINEERING

COLLEGE OF BIOLOGICAL AND CHEMICAL ENGINEERING

JUNE 2019

Approval Page

This is to certify that the thesis prepared by **Mr. Muluneh Ayalew Balcha** entitled **"Synthesis and Characterization of Cellulose Nanocrystals from Water Hyacinth using Acid Hydrolysis"** and submitted as a partial fulfilment for the award of the Degree of Master of Science in Chemical Engineering (Chemical process and Product Design) complies with the regulations of the university and meets the accepted standards with respect to originality, content and quality.

Signed by Examining Board:

Advisor: Signature, Date:

External Examiner: Signature, Date:

Internal Examiner: Signature, Date:

Chairperson: Signature, Date:

DGC chairperson: Signature, Date:

College Dean/Association Dean for GP: Signature, Date:

Declaration

I hereby declare that this thesis entitled **"Synthesis and Characterization of Cellulose Nanocrystals from Water Hyacinth using Acid Hydrolysis"** was prepared by me, with the guidance of my advisor. The work contained herein is my own except where explicitly stated otherwise in the text, and that this work has not been submitted, in whole or in part, for any other degree.

Author: Signature, Date

_____

Witnessed by:

Name of Students Advisor: Signature, Date

_____

Name of Student Co-advisor: Signature, Date

_____

Abstract

Water hyacinth is a widespread aquatic plant with extremely high growth rate which presented a big problem in the past and a tough challenge at present due to its ability to rapidly cover the whole water body. It poses serious socioeconomic and environmental problems over the world. Several biological, physical and chemical methods have been tried for the control and eradication of this plant from water bodies. However, none of these methods proved to be a permanent solution since the attempts to control it needs high costs and labour requirements. The aim of this study was to utilize this plant for production of cellulose nanocrystals (CNCs) using acid hydrolysis method at different values of hydrolysis temperature, time and acid concentration. Pretreatment steps such as soxhlet extraction, alkaline treatment and bleaching were performed for successful isolation of cellulose for acid hydrolysis. After acid hydrolysis, purified dispersion of CNCs was obtained using successive centrifugation, dialysis and ultrasonication. The effect of process parameters on the yield of CNCs was evaluated and optimized using response surface methodology (RSM). The raw water hyacinth, freeze dried cellulose and CNCs samples were characterized using scanning electron microscopy, X-ray diffraction, Fourier Transform Infrared Radiation, differential scanning calorimetry and particle size analyzer. It was found that the whisker-shaped structured CNCs was isolated with an average diameter of 102.6 nm and showing high thermal stability. It was also observed that the non-cellulosic components were successfully removed and the crystallinity index as well as crystal thickness of the sample was improved after each treatment. The yield of CNCs was affected by selected process parameters and the maximum yield of 37.72% was obtained at 50 ^{o}C, 35 min and 54% acid concentration and optimized to 38.4057 %.

Keywords: Water hyacinth; Nanocellulose; Acid Hydrolysis.

Acknowledgments

First and foremost, thanks to GOD for all the strength and presence of outstanding people around me. Next, I would like to express my sincere gratitude to my advisor Dr. Girma Gonfa for his excellent scientific guidance, patience, kindness, right encouragement from the beginning of this thesis and special help on preparing this document. I would also like to acknowledge all departments under the college of Biological and Chemical Engineering as well as central lab for their invaluable support on sample characterization. Special thanks to chemical engineering department and all academic and research assistants for their technical and material help during lab work. Finally, I wish to express my deepest gratitude to my parents and friends for their emotional support and encouragements.

Table of contents

List of Tables

List of Figures

List of Abbreviations and Acronyms

AVOVA	Analysis of Variance
BBD	Box-Behnken Design
BNC	Bacterial Nanocellulose
CNCs	Cellulose Nanocrystals
CNF	Cellulose Nanofibrillated
C_I	Crystallinity Index
D	Diameter
DP	Degree of Polymerization
I_{200}	Intensity of Crystalline Cellulose
I_{am}	Intensity of Amorphous Cellulose
M	Molarity
PSA	Particle Size Analyzer
RSM	Response Surface Method
T	Temperature
V	Volume
W1	Weight of Dried Cellulose after Hydrolysis
W2	Weight of Dried CNCs before Hydrolysis
Wt	Weight
WH	Water Hyacinth

1. Introduction

The development of more sustainable and environmental friendly materials obtained from renewable sources (biomass) has gained the attention of researchers at the international level (Kallel et al., 2016). Lignocellulosic biomass is the most abundantly available renewable raw materials for the chemistry of cellulose nanomaterials and is a prime candidate for replacing oil-based feedstocks as it has been summarized in many recent review papers and articles (Chen et al., 2015; Kargarzadeh et al., 2017; Malucelli et al., 2017; Oksman et al., 2016; Sindhu et al., 2017). Cellulose nanocrystals (CNCs) is an interesting material among cellulose nanomaterials in nanotechnology field for many applications due to its attractive properties (Paulo et al., 2013; Taflick et al., 2017). The specific properties of cellulose nanocrystalline includes excellent mechanical properties, high surface area to volume ratio, light weight and low density, rich hydroxyl groups for modification, a capacity to be acquired in different dimension such as aspect ratio, inexhaustibility and natural properties with 100% environmental friend (Abdul Latif & Mahmood, 2018; Chirayil et al., 2014; Malucelli et al., 2017; Mashego, 2016). Cellulose nanocrystalline can be one of the alternative solutions to make cellulose more easily to be modified and dissolved in water (Nasikin et al., 2013).

The surface of CNCs can be modified with various chemical treatments to any desired surface modification due to the abundant hydroxyl groups on the surface of CNCs which provide them reactive. This can successfully functionalize the CNCs and facilitate the incorporation and dispersion of CNCs into different polymer matrices (Mashego, 2016). Now a days, it shows a great potential in the various applications including a barrier in the separation process of hazardous waste, biomedical products, electronic sensors, paints and coatings, as the thickener in cosmetics, biodegradable package, CO_2 adsorbent, as filler of special textiles, food wraps and texturing agent which replace the non-biodegradable plastics, as fillers and rheology modifiers in different fields like foams, aerogels and polymer electrolytes (Marimuthu & Atmakuru, 2015; Taflick et al., 2017). It can also be used as nanocomposite materials in polymer science to improve mechanical, thermal and ionic conductivity properties of polymer (Endes et al., 2016; Malucelli et al., 2017; Phanthong et al., 2018).

For this interesting material, lignocellulosic biomass from different sources has become the most potential renewable and promising feedstock. This lignocellulosic biomass may include certain micro-organisms, higher plants, agricultural residues and certain animals from which cellulose can be extracted. Cell wall structure of these lignocellulosic biomasses mainly consists of components such as cellulose, hemicellulose, lignin and additionally some extractable components (Asrofi et al., 2018; Malucelli et al., 2017; Sindhu et al., 2017). Agricultural residues, forest residues and energy crops have been used as raw materials for cellulose nanocrystals (Lee et al., 2014). However, most of these lignocellulosic biomasses are obtained from seasonable and slow growing plants as well as utilizing for other purposes. Hence, finding of lignocellulosic biomass with fast growth rates, non-seasonable and less utilized for other purposes is more worthwhile with respect to the economic, environmental and ecological benefits (Yandan et al., 2015).

Water hyacinth is one of such lignocellulosic biomasses and therefore, can be used as a suitable feedstock for cellulose nanocrystals. It has extremely high growth rates and called the world's worst aquatic weed due to its ability to rapidly cover whole waterways (Soetaredjo et al., 2016; Thuyen et al., 2017). This leads to the formation of dense coverage that prevents the sunlight from penetrating the water and impenetrable mats over the water surface (Priya & Selvan, 2017; Teygeler, 2000). It can also forms other specific problems such as destruction of eco systems, blocking irrigation channels and rivers, destroying natural wetlands, eliminating native aquatic plants, reducing infiltration of sunlight, changing the temperature, pH and oxygen levels of water, reducing gas exchange at the water surface, increasing water loss through transpiration, restricting recreational use of waterways, and reducing water quality from decomposing plants (Pitaloka et al., 2013; Sunita and Narayan, 2010). Generally, many rivers, reservoirs and channels have been polluted and clogged by this plant and therefore, seriously affect the development of transport, tourism and aquaculture (Marimuthu & Atmakuru, 2015; Navarro & Phiri, 2000; Sanmuga Priya & Senthamil Selvan, 2017).

The negative effects of water hyacinth lead to several research and developmental activities for the control of this notorious weed. Several biological, physical and chemical methods have been tried for the control and eradication of water hyacinth. However, none of these strategies proved to be a permanent solution since the attempts to control this weed have

high costs and labour requirements (Sindhu et al., 2017). Thus, it is necessary to find a suitable way to utilize the water hyacinth, that is, by mechanically removing it from water bodies and producing value added materials from it. Water hyacinth has a high percentage of cellulose (Asrofi et al., 2018) and hemicellulose with low lignin content (30% to 44% cellulose , 24% to 26% hemicellulose, and 18% to 23% lignin) (Latif, 2018; Sivasankari., 2016; Soetaredjo et al., 2016) which is comparable with the fiber content from other sources, such as wood, rise husk, wheat straw, corn strove, pineapple leaf and etc. (Kasim et al., 2018; Latif, 2018; Lee et al., 2014; Marcos et al., 2013; Pitaloka et al., 2013). This comparable content of cellulose, its impressive growth rate and no completion on land use have led water hyacinth to be regarded as a good lignocellulosic material source for cellulose nanocrystals, which has a much higher economic value compared to the existing use of cellulose (Soetaredjo et al., 2016).

Different methods such as mechanical treatment, biological treatment (enzymatic hydrolysis), chemical treatment (acid hydrolysis), and the combination of any of these methods can be used to produce nanocellulose from lignocellulosic biomass (Ghazy et al., 2016; Lee et al., 2014; Phanthong et al., 2018; Wulandari, 2016). All these treatment methods lead to the different types of nanostructured cellulose molecules differing in dimension, degree of crystallinity and morphologies depending on their disintegration process and feedstocks (Bhat et al., 2017). However, high energy is required for the mechanical method and long time of operation and high cost is needed for enzymatic hydrolysis. In this study, acid hydrolysis was used for various reasons such as: it presents lower cost and good efficiency to obtain cellulose nanocrystals; it is easy and fast to produce nanocellulose that has better properties; it gives nanocellulose with higher crystallinity index and smaller size than other methods (El et al., 2018; Malucelli et al., 2017; Lee et al., 2016b). During acid hydrolysis, the most important factors to be controlled are acid concentration, reaction time and reaction temperature (Thambiraj & Ravi Shankaran, 2017). Different acids have been used for acid hydrolysis of lignocellulosic fibers. Among these, sulfuric acid (H_2SO_4) and hydrochloric acid (HCl) are the most common for hydrolysis purpose (Bhat et al., 2017; Malucelli et al., 2017). However, treatment with hydrochloric acid results in reduced dispersion of crystals, leading to flocculation in solution, lower crystallinity index due to its higher tendency to promote the

breakage of the hydrogen bonds in the crystalline region of cellulose (Malucelli et al., 2017). H_2SO_4 is the most common acid used for acid hydrolysis process since it produces CNCs particles grafted with the negatively charged sulfate ester group which makes the CNCs particles a negative electrostatic repulsion force. It stabilizes the nanocellulose suspension by electrostatic repulsion avoiding fibril aggregation (Abitbol et al., 2016; Malucelli et al., 2017; Mariño et al., 2015). In this study, cellulose nanocrystals were produced from water hyacinth using H_2SO_4 hydrolysis method and also the effects of reaction temperature, reaction time and acid concentration on the yield of CNCs were investigated and optimized using Response Surface Method (RSM). The obtained CNCs was characterized using different techniques.

1.1 Statement of problems

Water hyacinth is a widespread aquatic plant with extremely high growth rate. It presented a big problem in the past and a tough challenge at present due to its ability to rapidly cover the whole water body. It poses serious socioeconomic and environmental problems over the world. Degradation of ecosystem services including transportation, hydropower operations and fisheries were some of the direct effects of water hyacinth. Removal of this plant from water bodies comes with substantial costs. Several biological, physical and chemical methods have been tried for the control and eradication of this plant from water bodies. However, none of these methods proved to be a permanent solution since the attempts to control it needs high costs and labour requirements. In addition, further problems such as secondary contamination via nutrient leaching and greenhouse gas emissions occurred with disposal of water hyacinth biomass on landfill.

Hence, a practical way of management to remove water hyacinth from water body is to understand existing technologies and integrate them with further research for a useful application. Even though water hyacinth presented a big problem in the past and a tough challenge at present, it may be a potential opportunity in the future to be used as a suitable lignocellulosic feedstock for value added materials. In this study, it is used as lignocellulosic material source to produce cellulose nanocrystals due to its high contents of cellulose, impressive growth rate and no competition on land use. It would be more worthwhile to generate cellulose nanocrystals from this fast-growing renewable plant with respect to the economic and ecological benefits. Different methods such as mechanical,

biological and chemical treatments have been used for producing nanocellulose from lignocellulosic biomass. Sundari & Ramesh (2012) have extracted cellulose nanofibers from water hyacinth by mechanical treatment such as Ball milling, cryocrushing, high pressure homogenization and utrafine grinder which are more energy consuming techniques. Biological treatment (enzymatic hydrolysis) needs long time and high cost of operation. Compared to these methods, acid hydrolysis is the most common and best method to get cellulose nanocrystals with better properties. Asrofi et al. (2018) have isolated nanocellulose from water hyacinth via digester sonication and acid hydrolysis using hydrochloric acid. However, hydrolysis with hydrochloric acid results in reduced dispersion of crystals, leading to their flocculation when in solution. Therefore, this work was aimed to produce cellulose nanocrystals from water hyacinth using sulfuric acid as hydrolyzing agent; investigate the effects of hydrolysis temperature, time and acid concentration on the yield and characterize the obtained CNCs using different techniques.

1.2 Objectives

1.2.1 General objective

The aim of this study was to produce and characterize cellulose nanocrystals from water hyacinth using H_2SO_4 hydrolysis method.

1.2.2 Specific objectives

a) To isolate and purify cellulose from water hyacinth fiber using appropriate solvents.
b) To characterize purified cellulose.
c) To synthesis cellulose nanocrystals using H_2SO_4 hydrolysis and investigate the effects of acid concentration, reaction temperature and time on the yield of CNCs.
d) To characterize the synthesized cellulose nanocrystalline.

1.3 Significance of the study

After successful completion, this research can be used in different ways for the whole environment. Since water hyacinth is renewable resource, its utilization can contribute to the solution of socio-economic problems associated with it. In one way it will be used for the removal of water hyacinth from water bodies and also reduce disposal in a landfill. As a result, it will contribute in keeping the aquatic ecosystem and overall environment safer. Similarly, the utilization of water hyacinth will be used for industries to reduce the cost of raw materials for nanocellulose production and enhance benefits by converting this

abundantly available raw material to value added products rather than disposal in a landfill. For the researcher it will provide opportunities to increase the practical knowledge. Furthermore, for the University it will help to promote its mission and build up the link with the industry.

1.4 Scope of the study

This work concentrates on the basic study of water hyacinth utilization for production of cellulose nanocrystals. First, cellulose isolation and purification was carried out using Soxhlet extraction, alkaline treatment and bleaching as pretreatment steps. Next, obtained purified cellulose was freeze dried and characterized. Then, cellulose nanocrystal was synthesized via H_2SO_4 hydrolysis at different reaction temperature, reaction time and acid concentration. The obtained CNCs was purified using successive centrifugation and membrane dialysis. Finally, the suspension of CNCs was ultrasonicated to get homogenized dispersion, freeze dried and characterized. The effects of process parameters on the yield of CNCs were investigated and optimized using Response Surface Method.

2. Literature Review

2.1 Lignocellulosic Materials

Lignocellulosic biomass is one of the major renewable resource materials throughout the world and includes various natural organic matters which mostly refer to the plants (Chirayil et al., 2014). Lignocellulosic biomass industry has become green, possible alternative of fossil resources in order to compensate the increasing trend of world's demand for petroleum usage (Yahya et al., 2015). It is the largest amount of sustainable carbon material group and the most promising feedstock for the sustainable production of high value-added materials (Chen et al., 2015; Chirayil et al., 2014; Kargarzadeh et al., 2017; Lee et al., 2014; Malucelli et al., 2017; Oksman et al., 2016; Phanthong et al., 2018; Sindhu et al., 2017). There are many species of useful fibre plants in various parts of the world which are used for many applications. It is estimated that the worldwide production of lignocellulosic biomass is about 1.3×10^{10} metric tons per annum (Santos et al., 2013). These lignocellulosic resources may include (i) agricultural residues (palm trunk and empty fruit bunch, corncobs, wheat straw, sugarcane bagasse, corn stover, coconut husks, wheat rice, and empty fruit bunches); (ii) forest residues (hardwood and softwood); (iii) energy crops (switch grass); (iv) food wastes; and (v) municipal and industrial wastes (waste paper and demolition wood) (Lee et al., 2014). Changing of these low cost and abundantly available lignocellulosic materials to products with superior functions presents a feasible option for improvement of energy security and greenhouse emission reduction. It can be considered as main source for the production of biofuel (Soetaredjo et al., 2016), biochemicals, biopolymer materials and other value added products for economical and sustainable development (Fortunati et al., 2016; Herrera Rodriguez, 2015; H. V Lee et al., 2014). Lignocellulosic fibers are excellent raw materials for the chemistry of polymers and composites, which can be proven by the high number of patents and national and international articles, besides the large number of products already marketed (Sá, Miranda, & José, 2016). The materials obtained from the renewable bio-resources could be the alternative of petroleum based synthetic products due to their advantages of relatively low cost, environmental friendly in nature, easy availability, renewability, and nontoxicity (Mondal, 2017). Among these materials, cellulose based nanomaterials derived from renewable lignocellulosic biomass could play a significant role in the nanotechnology

research domain (Fortunati et al., 2016). In this concept, the preparation of novel, low-cost and high-performance cellulose nanomaterials (nanocellulose) from renewable and sustainable resources is an expanding research area and is getting attention in the recent decade since it offers unique physiochemical properties (Liu et al., 2016; Mondal, 2017). Many agricultural and industrial wastes have attracted much attention in the extraction and utilization of nanocellulose in recent years.

2.2 Composition of lignocellulosic materials

Cell wall structure of lignocellulosic biomass mainly consists of components such as cellulose, hemicellulose, lignin and additionally some extraneous substances (Asrofi, Abral, Kasim, Pratoto, Mahardika, Park, et al., 2018; Fortunati et al., 2016; Hutomo, Rahim, & Kadir, 2015; Y. Jiang et al., 2017; Malucelli et al., 2017; Mishra, Sabu, & Tiwari, 2018; Sindhu et al., 2017). The composition and the content of these components are varied depending on the difference in species, types, and sources of lignocellulosic materials (Abdul Khalil et al., 2016). Most of the lignocellulosic biomasses are comprised of about 10-25% lignin, 20-30% hemicellulose, and 30-50% cellulose (Fortunati et al., 2016; Phanthong et al., 2018). Lignocellulosic materials that have higher cellulose content with low hemicellulose and lignin are a suitable feedstock for the production of cellulose based materials. Cellulose molecule, which is the major structural component of plant cell wall, arranged regularly, gathered into bundles, and determines the framework of the cell wall (Fortunati et al., 2016). Cellulose and lignin in lignocellulosic biomass and are surrounded by hemicellulose chains. There are different bonding among cellulose, hemicellulose and lignin (Rezania et al., 2017). These molecules are mainly coupled by a hydrogen bond. In addition to the hydrogen bond, there is also the chemical bonding between hemicellulose and lignin, which results in the lignin, isolated from natural lignocelluloses, always contains a small amount of carbohydrates. Other components of lignocellulosic biomass are an extraneous component which refers to all the non-cell wall materials. The extractives can be crudely divided into three groups, namely, terpenes, resins, and phenols. The resins include a wide variety of non-volatile compounds, including fats, fatty acids, alcohols, resin acids, phytosterols, and less known neutral compounds in small amounts. Other extractives include low molecular weight carbohydrates, alkaloids, and soluble lignin. In spite of the fact that they exist in small quantities, extraneous compounds play a very

significant role in that they render cellulose not only resistant to decay and insect attack but also inhibitive to pulping and bleaching. Generally, the relative abundance of cellulose, hemicellulose, and lignin is the key factor in determining the feedstock suitability for nanocellulose production (Phanthong et al., 2018). During nanocellulose production, all of these components except cellulose are degraded and removed at different steps using appropriate solvents (Malucelli et al., 2017; Sindhu et al., 2017). In different studies, it was shown that the composition of these components varies depending on species, types, and their sources. Generally, the chemical composition of different types of common lignocellulosic materials is shown in Table 2.1.

Table 2.1. Chemical composition of common lignocellulosic materials

Lignocellulosic materials	Composition (%)			References
	Cellulose	Hemicellulose	Lignin	
Corn stover	39-44.4	22-28	18-22	(Krietemeyer et al., 2018)
Humulus japonicus stem	43.11	22.95	20.24	(Y. Jiang et al., 2017)
Sugarcane bagasse	45	30	20-22	(Oliveira, Bras, Pimenta, Curvelo, & Belgacem, 2016)
Arecanut husk fibre	34.18	20.83	31.6	(Georgeet al., 2016)
Garlic straw residues	41	18	6.3	(Kallel et al., 2016)
Coconut fiber	31–32	25–26	33–37	Nascimento et al. (2016)
Water Hyacinth stems	29.4 -33	24.6 - 28.35	18.36 - 23.8	(Sivasankari., 2016; Soetaredjo et al., 2016)
Lotus Leaf Stalk Agro-wastes	34.6	19.2	25.4	(Yandan et al., 2015)
Hardwood stem	40-45	24-40	18-25	Wustenberg **(**2015)
Softwood stem	45-50	25-30	25-35	
Oil palm frond	40-50	34-38	20-21	(Yahya et al., 2015)
Oil palm trunk	29-37	12-17	18-23	
Barley straw	33-40	20-30	8-17	(Lee et al., 2014)
Corncobs	45	35	15	
Empty fruit bunch	41	24	21.2	
Switch grass	45	31.4	12	
Nut shells	25-30	25-30	30-40	
Wheat straw	30	50	15	
pineapple leaf	34-40	21-25	25-29	(Santos et al., 2013)**,**

2.2.1 Hemicellulose

Hemicellulose is an amorphous heterogeneous polysaccharide that composed polymer of pentoses (xylose and arabinose), hexoses (mannose, glucose, and galactose) and acetylated sugars (Yahya et al., 2015). Hemicellulose acts as a compatibilizing agent, forming an interface between hydrophobic lignin and hydrophilic cellulose, and it links with cellulose and lignin in plant fibre cells. Hemicellulose represents about 20-30% in lignocellulosic biomass which adheres to the cellulose fibrils through hydrogen bonds and Van der Waal's interactions and also cross-links with lignin (Phanthong et al., 2018). Hemicellulose can be hydrolyzed by acid, alkali, or enzymes in mild conditions for production of fuel ethanol and the valuable chemicals from its oligomers or monomer (Fortunati et al., 2016; Phanthong et al., 2018). It can be applicable barrier materials for packaging and in cosmetics, in mining industries as biopolymers with new properties.

2.2.2 Lignin

Lignin is defined as an amorphous three-dimension complex heteropolymer that composed of propyl–phenol groups linked by C–C bonds and an ether group. It consists of the cross-linked amorphous copolymer and serves as the binder which holds between cellulose and hemicellulose complexion (Lee et al., 2014). With its binding function, lignin provides the stiffness, compressive strength, resistant to decay, resistance to microbial attack, oxidative stress and water impermeability to plant cell wall to act as physical protective barrier for plant cell wall (Abdul Khalil et al., 2016; Phanthong et al., 2018; Yahya et al., 2015). Basically, softwood consists of higher amount of lignin compared to other types of biomass which makes soft wood more recalcitrant and resistant than the other feedstock in cellulose separation step. Removal of lignin is an important process to cause biomass swelling, disruption of lignin structure, increase in internal surface area, and increase accessibility of hydrolysis reaction. It can serve as a future aromatic source for the green chemicals used as building block for polymer such as polyester and polyurethanes due to its large quantities of poly-aromatic structure (Yahya et al., 2015).

2.2.3 Cellulose

Cellulose is one of the most abundant renewable biopolymer resources on earth (Malucelli et al., 2017) and is found in various organisms, including higher plants, bacterial, marine algae and certain animals (Lee et al., 2016). It is a natural high molecular component of

lignocellulosic biomass which is mainly localized in the plant cell wall at around 32-50% (Kasim et al., 2018; Latif, 2018; Lee et al., 2014). It is a product of the photosynthesis process in plant with the molecular formula of $(C_5H_{10}O_5)_n$ (Yahya et al., 2015) and is an important structural component of plant cell walls which determines its mechanical properties (Bhat et al., 2017; George, 2015). Plants are the potential main sources of cellulose because they are abundant and relatively cheap. A wide variety of plant materials such as jute, ramie, sisal, flax, hemp, water plants, grasses, and some parts of plants such as leaves, stem, fruit, etc. are well known sources for cellulose production. Agricultural wastes such as wheat and rice straw, sugarcane bagasse, sawdust, cotton stables, etc. are also used for the production of cellulose. The total annual amount of cellulose production is estimated at over 7.5×10^{10} tons of total annual biomass production (Fortunati et al., 2016) and is considered as a prime candidate for replacing oil-based feedstocks due to its reinforcement properties (Endes et al., 2016; Khawas & Deka, 2016; Mashego, 2016; Wulandari, 2016). It has been widely used in different fields such as manufacture of pulp and paper, chemical materials as well as building materials. Recently, the use of cellulose as raw materials for bio-energy and eco-friendly polymer materials has investigated by different studies.

It is a linear polymer of dimer of glucose known as cellobiose with a long chain and a high molecular weight of approximately more than 500,000 Da (Fortunati et al., 2016; Wulandari et al., 2016). The number of chain units, the so-called degree of polymerization (DP) varies for different cellulosic materials depending on their source. Normally commercially available cellulose has degree of polymerization about 983.40 units of anhydrous glucose and molecular weight about 159.408 (Hutomo et al.,2015). It is also estimated to be about 10,000 gluco-pyranose units in wood cellulose and 15,000 units in native cotton depending on its origin (Fortunati et al., 2016). Individual glucose molecules are linked together by β-1, 4 bonds to form a highly crystalline material and its chains tend to be very close to each other (Kumar et al., 2018; Lee et al., 2014; Mashego, 2016). Naturally occurring cellulose does not occur as an isolated individual molecule, but rather it is found as assemblies of individual cellulose chain-forming fibres (Mishra et al., 2018; Yahya et al., 2015). The fibrils in which these are orientated determine the morphological hierarchy, which pack into larger units called micro fibrils, which are in turn assembled

into fibre (Abdul Khalil et al., 2016; Bhat et al., 2017). These micro fibrils have disordered (amorphous) regions and highly ordered crystalline regions (George & S N, 2015). In the crystalline region, cellulose chains are closely packed together or assembled via complex intra- and inter-molecular hydrogen bond network which allow them to be packed side by side in planar sheet and bundled into micro fibrils (Bhat et al., 2017; Endes et al., 2016; Mashego, 2016; Yahya et al., 2015). This leads the polymer to be stable and crystalline structure, which is its basic characteristic and positive factor that could be used for better results in relation to structural reinforcement (Lee et al., 2016a; Malucelli et al., 2017). The chemical composition and conformation of cellulose chains combined with their hydrogen bonding system are responsible for their tendency to form crystalline aggregates (Phanthong et al., 2018). The amorphous regions in cellulose microfibrils are weak and thus easily breakdown into shorter crystalline part when lignocellulosic biomass subjected to de-polymerization treatments. Cellulose poses low density, , nonabrasive, combustible, nontoxic, low cost, biodegradable and has good thermal and mechanical properties (Khawas & Deka, 2016; Wulandari, 2016).

The cellulose molecule is a linear polymer of D-anhydroglucopyranose units linked together by β-1, 4-glucosidic bonds (Malucelli et al., 2017; Phanthong et al., 2018). The conventional numbering of the carbon atoms in cellulose ring is shown in Fig. 2 where positions 1 and 4 are involved in the inter-unit linkage. In the cellulose chain, the glucose units are in 6-membered rings, called pyranoses. They are joined by single oxygen atoms between the C-1 of one pyranose ring and the C-4 of the next ring. C1 is an acetal centre along the whole chain except for the right-hand end where it is a hemiacetal centre with inherent reducing properties. Thus, cellulose has one reducing end containing an unsubstituted hemiacetal, and one non-reducing end containing an additional hydroxyl group at C4. Since a molecule of water is lost due to the reaction of an alcohol and a hemiacetal to form an acetal, the glucose units in the cellulose polymer are referred to as anhydroglucose units (Xie et al., 2016). The spatial arrangement or stereochemistries of these acetal linkages are very important. The pyranose rings of the cellulose molecule have all the groups larger than hydrogen sticking out from the periphery of the rings (equatorial positions). Because of the equatorial positions of the hydroxyls on the cellulose chain, they

protrude laterally along the extended molecule and are readily available for hydrogen bonding.

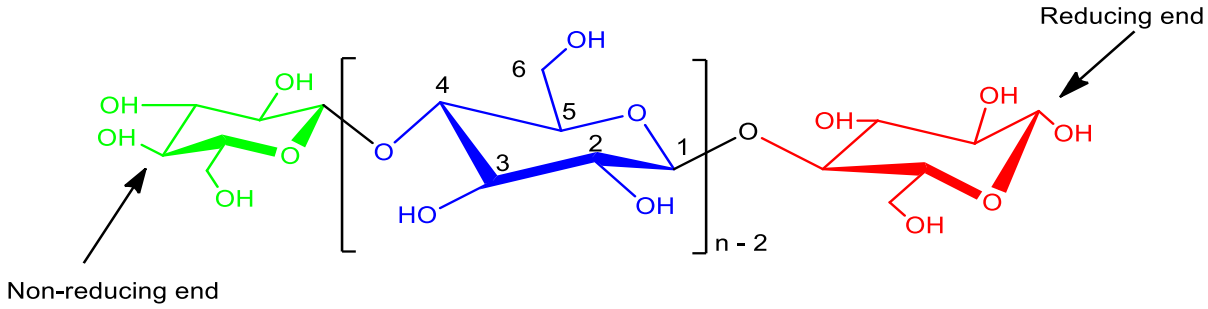

Figure 2.1. Molecular structure of cellulose showing the numbering of the carbon atoms (Fortunati et al., 2016).

Anhydroglucose unit consists of three hydroxyl groups which form strong hydrogen bond with the adjacent glucose unit in the same chain and with the different chains, called as intramolecular and intermolecular hydrogen bonding networks, respectively (Phanthong et al., 2018; Wulandari et al., 2016). These hydrogen bonding networks are strong and tightly packed in the crystalline parts of cellulose fibrils which lead cellulose some of the characteristic properties such as hydrophilicity, chirality, biodegradability, toughness, strength, fibrous, highly cohesive nature and high resistant to most organic solvents in plant cell wall, which are initiated by the high reactivity of the hydroxyl groups (George & S N, 2015). The hydrophilic nature of cellulose macromolecules is due to the three-alcoholic hydroxyl (–OH) groups. Therefore, an unbonded hydroxyl group that mainly presents in the amorphous region of cellulose plays a major role in their reactive nature during the hydrolysis process, whereas the crystalline region of cellulose remains intact. They also prevent cellulose from melting (non-thermoplastic). Most cellulose structures can absorb large quantities of water (hygroscopic) and therefore cellulose swells but does not dissolve in water (Xie et al., 2016). However, strong acids, strong alkalis, concentrated salt solutions, and various complexing reagents can swell or disperse and even dissolve the cellulose. The glucose molecules and hydrogen bonding networks in cellulose has wide orientation, resulting in different allomorphs of cellulose. The variation of cellulose allomorphs depends on the source of lignocellulosic biomass and the treatment method (Phanthong et al., 2018).

2.3 Water hyacinth

Water hyacinth (*Eichhornia crassipes*) is a large free floating vascular macrophyte, perennial and widespread aquatic plant species belongs to family Pontederiaceae. It originated from Amazon River basin and have distributed throughout the world (Pitaloka et al., 2013; Soetaredjo et al., 2016). The water hyacinth was first recorded as a separate species by the explorer of tropical South America Martius in 1824 and it is a noxious, unique, fast growing and persistent invasive macrophyte (Navarro & Phiri, 2000; R., 2000; Sanmuga Priya & Senthamil Selvan, 2017). The growth rate of water hyacinth is estimated to be 220 kg/ha per day. Water hyacinth have caused extensive damages due to its biology and function in the aquatic ecosystem, with the technology of its control and management not fully understood (Thuyen et al., 2017). The main characteristics of the biology of the macrophyte can be summarized as: morphological elasticity, extremely fast growth rate, changing chemical composition of different parts of plant in various habitats, adaptive phenology for ecological invasion, and vegetative and sexual reproduction for persistent distribution. These basic characteristics and the interactions of this species with the environment, including temperature, light, pH, dissolved oxygen and salinity are well described. However, over the decades, new characteristics and behaviors of the plant have been explained to assist in-depth understanding of this macrophyte, and to help deal with environmental challenges, management and control of the species and utilization of its biomass (Akendo et al., 2008).

(Navarro & Phiri, 2000), did a survey of problems and solution on water hyacinth in Africa and Middle East. Water hyacinth has exhibited extremely high growth rates and called the world's worst aquatic weed due to its ability to rapidly cover whole waterways (Soetaredjo et al., 2016; Thuyen et al., 2017). This leads to the formation of dense coverage that prevents the sunlight from penetrating the water and impenetrable mats over the water surface (Priya & Selvan, 2017; Teygeler, 2000). It poses serious socioeconomic and environmental problems for millions of people which add constraint on development (Abdul Latif & Mahmood, 2018; Marimuthu & Atmakuru, 2015). It can also forms other specific problems such as destruction of eco systems, blocking irrigation channels and rivers, restricting livestock access to water, destroying natural wetlands, eliminating native aquatic plants, reducing infiltration of sunlight, changing the temperature, pH and oxygen

levels of water, reducing gas exchange at the water surface, increasing water loss through transpiration, altering the habitats of aquatic organisms, restricting recreational use of waterways, reducing aesthetic values of waterways, and reducing water quality from decomposing plants (Pitaloka et al., 2013; Sunita et al., 2010; Yan, 2016)

Over the last few decades, a lot of experience has been acquired about various methods of control, such as mechanical removal, chemical herbicides and the introduction of natural predators (Navarro & Phiri, 2000; Sindhu et al., 2017). However, this method of integrated pest management probably won't achieve the definitive and total eradication of the water hyacinth (Navarro & Phiri, 2000). Part of an integrated programme could be the search for a useful application for the plant in question (Teygeler, 2000). This is why useful applications are now being sought for the water hyacinth. Already many possibilities have been investigated such as a food source for animals, as a fertilizer, as fibre or cellulose source, as raw material for paper making and the like (Navarro & Phiri, 2000; Sindhu et al., 2017; Soetaredjo et al., 2016). The evaluation of water hyacinth composition is important due to the variation of carbohydrate and lignin content in different studies. Sivasankari & David Ravindran (2016) studied the chemical composition of water hyacinth on dry weight basis. According to this study, it was reported that the stem of water hyacinth contains 29.33% cellulose, 28.35% hemicellulose and 18.36% lignin. Pitaloka et al. (2013) also reported that water hyacinth has a high percentage of cellulose and hemicellulose (44% to 66.9% of dry weight basis) and low lignin content from 5% to 9.5%. The percentage of chemical composition in water hyacinth had also presented by another study as: cellulose (29.4 to 53.3)wt%, hemicellulose (22.7 to 24.6)wt% and lignin (8.9 to 23.8)wt% (Soetaredjo et al., 2016). High contents of cellulose and hemicellulose with low lignin, impressive growth rate and no competition on land use have led water hyacinth to be regarded as a suitable lignocellulosic material for the production of high value-added materials using different chemical and mechanical treatment (Priya & Selvan, 2017; Sivasankari et al., 2016; Soetaredjo et al., 2016).

2.4 Production of Nanocellulose and its Application

2.4.1 Introduction

Nanocellulose refers to a biodegradable natural nanomaterial which can be extracted from plant cell wall cellulose by means of chemical or mechanical treatment with at least one

dimension in the nanometer scale range (Bhat et al., 2017). The nanoscale dimension and its capacity to form a strong entanglement of nanoporous networks have changed the emergence of new high-value applications. The special attention is the size of nanocellulose fiber which generally contains less than 100 nm in diameter and several micrometers in length (Phanthong et al., 2018). Due to its unique reinforcement properties, nano sized cellulose fibers have attracted more and more interest in recent decades for different promising applications (Morais et al., 2013; Yandan et al., 2015). The functions and structural properties of the nanocellulose are highly dependent on the cellulose source and preparation process. Nanocellulose can be categorized into three main types; cellulose nanocrystalline (CNCs), cellulose nanofibrillated (CNF), and bacterial nanocellulose based on their dimension, preparation methods, and cellulosic source to render themselves for the specific application (Abitbol et al., 2016; Bhat et al., 2017; Yahya et al., 2015). Although all types are similar in chemical composition, they are different in morphology, particle size, crystallinity, and some other properties due to the difference of sources and extraction methods (Phanthong et al., 2018).

Cellulose nanofibrillated (CNF) refers to the long, flexible, and entangled cellulose fibers that have been fibrillated and produced through mechanical methods to achieve agglomerates of cellulose microfibril units. It has the long fibril shapes with nanoscale (less than 100 nm) diameter and 500–2000 nm in length (Bhat et al., 2017; Missoum et al., 2013). It contains a large amount of amorphous cellulose, while surface morphologies and dimensions of CNF can vary substantially, depending on the degrees of fibrillation and any pre-treatment involved. Nanofibrillated cellulose displays two main drawbacks, which are associated with its intrinsic physical properties. The first one is the high number of hydroxyl groups, which lead to strong hydrogen interactions between two nanofibrils and to the gel-like structure once produced. The second drawback is the high hydrophilicity of this material, which limits its uses in several applications such as in paper coating (increase of dewatering effect) or composites due to its tendency to form agglomerates in petro-chemical polymers (Missoum et al., 2013). The most feasible solution to this is chemical surface modification to reduce the number of hydroxyl interactions and also to increase the compatibility with several matrices. Because of their promising characteristics, nanofibrillated cellulosic fibres have been widely utilized in a variety of applications in

various fields such as medical, packaging, paper and coating, electronics and membranes (Abdul Khalil et al., 2016).

Cellulose nanocrystalline (CNCs), also known as cellulose nanowhiskers, is the short-rod-like shape with 2–100 nm in diameter and 100–500 nm in length. It has high degree of crystallinity that can vary from 65 to 95%, giving high strength. However, their lengths and diameters, degree of crystallinity and morphology may vary, depending on the raw material and extraction process used (Bhat et al., 2017; Herrera Rodriguez, 2015). Cellulose nanocrystals are the highly ordered crystalline region in cellulosic materials which are usually produced from cellulose fibrils through acid hydrolysis by removing the amorphous region of the cellulose chain (Bhat et al., 2017; Malucelli et al., 2017). Due to its desirable properties such as high degree of crystallinity, this crystalline part of the cellulose has captured the attention of the materials science community. Recently cellulose nanocrystals proved to be a useful material on which to base a new polymer composite industry. The nanoscale dimension and its capacity to form a strong entangled nanoporous network have changed the emergence of new high- value applications. The abundant hydroxyl groups on the surface of CNCs render them reactive and the surface of CNCs can be modified with various chemical treatments to any desired surface modification. These surface modification may include; esterification, etherification, oxidation, silylation, or polymer grafting, which could successfully functionalize the CNCs and facilitate the incorporation and dispersion of CNCs into different polymer matrices (Mashego, 2016).

Bacterial nanocellulose (BNC) is another kind of nanocellulose which is different from nanocrystalline cellulose and nanofibrillated cellulose. Nanocrystalline and nanofibrillated celluloses can be extracted from lignocellulosic biomass (top-down process) but bacterial nanocellulose is produced from building up of low molecular weight of sugars by bacteria (bottom-up process). The bacterial nanocellulose is always in the pure form without other components from lignocellulosic biomass such as lignin, hemicellulose, and pectin. Bacterial nanocellulose has the same chemical compositions as other two kinds of nanocellulose. It is in the form of twisting ribbons with the average diameters of 20–100 nm and micrometer lengths with large surface area per unit.

2.4.2 Methods of Nanocellulose Extraction from lignocellulosic biomass

As described above nanocrystalline cellulose can be prepared from various lignocellulosic materials. Due to the outstanding properties of nanocellulose and possibility for the future applications, the study of nanocellulose extraction from lignocellulosic biomass is very attractive. Biomasses such as waste cotton (Wang et al., 2017), sugarcane bagasse (Mashego, 2016; Wulandari, 2016), garlic straw residues (Kallel et al., 2016), agricultural waste corn stover (Xu et al., 2018), corncob residue (Liu et al., 2016) and others have been studied and used as the source of cellulose for nanocellulose production. However, most of these lignocellulosic biomasses are obtained from slow growing and seasonable plants which could also be used for other purposes. Therefore, it would be more worthwhile to produce nanocellulose from fast growing and non-seasonable plants as well as plants that could less utilizable for other purposes with respect to the economic and ecological benefits. Water hyacinth is one of such plants with rapid growth rates and hence, it is a more significant and promising source for production of nanocellulose. There are different extraction methods that have been used to obtain the nanocellulose with high crystallinity and surface area by breaking up the glycosidic bonds of cellulose molecules (Marimuthu & Atmakuru, 2015; Oun & Rhim, 2016). These methods include: mechanical treatment, biological treatment(enzymatic hydrolysis), chemical (acid hydrolysis), and the combination of any of these methods (Ghazy et al., 2016; Lee et al., 2014; Phanthong et al., 2018). All these treatment methods lead to the different types of nanostructured cellulose molecules differing in dimension, degree of crystallinity and morphologies depending on their disintegration process and initial source (Bhat et al., 2017).

2.4.2.1 Mechanical treatment methods

Mechanical process is the isolation of cellulose fibrils by applying high shear force to cleavage the cellulose fibers in longitudinal axis using different approaches. These mechanical approaches that have been utilized to obtain cellulose nanofibers (CNF) includes: high-pressure homogenizations, high-intensity ultrasonic treatments, micro fluidization techniques, ball milling methods, cryocrushing and grinding. These mechanical processes produce enough shear forces to split apart the cellulose fibers along the longitudinal axis and help to extract the cellulose microfibrils. Each cellulose microfibril is devoid of chain folding and can be considered a string of cellulose crystals,

linked along the microfibril by disordered or paracrystalline regions. High-pressure homogenizations result high amount of clogging, need pretreatment to reduce fiber size and prevent from clogging. It is quick, effective, continues process and reproducibility of laboratory results in ease of scale up to industrial scale. There is also possibility of finding right degree of defibrillation by varying pressure. However, high-pressure homogenizations require great energy consumption, high passing time though homogenization and increasing of suspension temperature during procedure. Micro-fluidization is advantageous due to less clogging, uniformity in reduction of sample size and fewer cycle are need to optimize fiber processing. But it is inappropriate for industrial scale. High-intensity ultrasonic treatment gives high power output and high efficiency of defibrillation. However, this method generates heat that must be dissipated and high level of noise. It also needs pretreatments to release CNF and only useful for laboratory scale (Abdul Khalil et al., 2016). Generally, the main drawback of all mechanical process is the high energy consumption and therefore the mechanical process is must need combination with other pretreatment method for decreasing energy (Phanthong et al., 2018).

2.4.2.2 Biological treatment method

Enzymatic hydrolysis is the biological treatment process in which enzymes are used for digesting or modifying cellulose fibers and conducted using mild conditions. Biological treatment is low energy requirement, environmentally friendly, has higher yields and higher selectivity. Micro-organisms such as brown, white, and soft rot fungi and bacteria are also used in biological treatment to degrade lignin and hemicelluloses from lignocellulosic material. However, long time of operation and high cost is needed for biological treatment because of enzymes and other micro-organisms used. Therefore, biological hydrolysis always needs incorporation with other methods such as mechanical shearing and high-pressure homogenization, leading to a controlled fibrillation down to the nanoscale, to produce cellulose nanomaterials (Bhat et al., 2017).

2.4.2.3 Chemical treatment method

Chemical treatment is the most promising method of preparing nanocellulose especially cellulose nanocrystalline. The chemical method produces rod-like short nanocrystals with improved crystallinity by reducing energy consumption and is better than other methods. Chemical method includes; alkali pretreatment, oxidizing agent, acid hydrolysis, and ionic

liquids pretreatment. Among them acid hydrolysis is the most commonly used method to prepare cellulose nanocrystalline due to its moderate operating conditions and good stability of the resulting suspension. During acid hydrolysis, the amorphous domains that are regularly distributed along the cellulosic fibers could be destroyed. Strong acids can easily penetrate into the amorphous regions having a low level of order and hydrolyze them under controlled conditions, leaving the crystalline regions unaffected. Nanocellulose extraction from lignocellulosic biomass through chemical method consists of two main steps. Firstly, the non-cellulosic components, such as lignin, hemicellulose, and other extractive compounds are removed by different pretreatment methods. Then, nanocellulose is extracted from cellulose fibrils by acid hydrolysis (Bhat et al., 2017; Ghazy et al., 2016; Lee et al., 2014; Phanthong et al., 2018; Taflick et al., 2017).

2.4.2.3.1 Pretreatment of biomass

Nowadays, the lignocellulosic biomasses are attractive for being the source of nanocellulose production. Not only it is high available in nature, but also the using of these biomasses can improve the value from non-valuable wastes to high profits of nanocellulose. As indicated above, lignocellulosic biomass consists of cellulose and non-cellulosic materials. The pretreatment of biomass is necessary step to ensure the separation of cellulose component from tight bond of polymeric constituents (cellulose, hemicellulose, and lignin) in lignocellulosic biomass (Sindhu et al., 2017). It removes other non-cellulosic components such as lignin, hemicellulose and some extractive components from cellulosic materials. The main intention of this fractionation treatment is to increase the accessibility of cellulose fiber to chemical attack prior to mild hydrolysis of isolated cellulose, by cleaving the ether bond between glucose chains in order to produce nano-size cellulose intermediate (Phanthong et al., 2018). However, biomass fractionation is a very complex process as high recovery of polysaccharides (cellulose, hemicellulose, and lignin) is required so that all three components can be fully converted into useful end products. Sometime, the biomass pretreatment shall lead to over de-polymerization of polysaccharide chains and subsequent sugar ring opening, which produce undesirable product such as glucose, acid, alcohol, and aldehyde. But such separation is mandatory step to unlock the stored fiber for effective utilization of nanocellulose in the current nanotechnology field (Sindhu et al., 2017).

The fractionation of lignocellulosic feedstock is probably the single most crucial step in the biorefinery process because it has a large impact on the yield and efficiency of the subsequent treatments and the quality of the obtained components (Fortunati et al., 2016). The pretreatment of biomass aims to reduce the degree of polymerization of cellulose by breaking the lignocellulosic complex which solubilize lignin and hemicellulose, increase porosity and surface area of hidden cellulose and reduce crystallinity of cellulose. This process improves de-polymerization of cellulose chain into nano dimension. The possible classical methods for biomass pretreatment are extraction, alkaline treatment and bleaching which can be acidic, alkaline and neutral (organosolv and ionic liquid treatments) in terms of pH. It involves a series of processes that may start with solvent extraction using solvents of different polarities to remove various extractives. Extractives are components of low molecular weight that includes a wide range of substances such as lignans, tannins, fats, waxes, alkaloids, proteins, simple and complex phenolic, simple sugars, pectins, gums, starch, glycosides and essential oils. The composition and amount of the extractives depend on the factors such as material species, age, and location (Taflick et al., 2017). Next to extraction step, the selective removal of lignin and hemicellulose from the fiber is done using different pretreatment methods. The possible chemical processes that can be used for pretreatment of lignocellulosic biomass includes dilute and concentrated acids (sulfuric acid, phosphoric acid, acetic acid and the like), alkaline (such as sodium hydroxide, calcium hydroxide), organosolv (mixtures of organic solvent and water), ionic liquids (e.g. Imidazolium salts) and oxidative such as hydrogen peroxides (Yahya et al., 2015).

These chemical processes for lignocellulosic biomass pretreatment have their own advantages and disadvantages. Although the main goal of pretreatment is to acquire a good quality cellulose product, it is important to preserve the structure of lignin and hemicellulose as well (Fortunati et al., 2016). Organosolv treatment is the best way to maintain high recovery of high quality and sulfur free lignin for specialty chemical process since it reduces the degradation of aromatic compounds. It is selective pretreatment method in which size reduction is of biomass feedstock is not necessary and also organic solvent used can be recycled and reused. However, the containment vessels to prevent leakage of volatile organic solvents and high cost of chemicals is needed. Other than solvent process, alkaline route with the presence of oxidation agent is another potential route to highly

solubilize lignin and hemicellulose with minimum formation of inhibitors. It is especially suitable for direct fermentation of sugar to bioethanol. But, it leads to alteration of lignin structure and also needs high cost of chemicals (Yahya et al., 2015). Alkaline treatment is generally carried out to partially solubilize hemicellulose fraction from fibers. It is used in order to expose cellulose crystals for further processing and enhances crystallinity structure (Fortunati et al., 2016). For alkaline pretreatment strong bases such as NaOH, KOH, Ca $(OH)_2$, hydrazine, and ammonium hydroxide are used under varying conditions as a pretreatment agents (Bhat et al., 2017). The most widely used alkaline is sodium hydroxide (4–20 wt %), which is always stirred with holocellulose for 1–5 h. Alkaline Pretreatment is usually conducted under mild conditions (below 140°C) as compared to other pretreatment technologies. During the pretreatment intermolecular ester bonds, which crosslink Xylan (hemicelluloses) and lignin, are subsequently saponified to increase their porosity. Then, the obtained solid products are washed by distilled water until reaching the neutral pH and finally dried in an oven at temperature below 50 ^{o}C. The obtained fiber products from this treatment are mainly in the form of cellulose after other noncellulosic materials have been removed (Phanthong et al., 2018). In case of direct acid treatment, a controllable amount of acid is the key point to solubilize cellulose and hemicellulose compounds. However, it is unsuitable to be used for fractionation of cellulose as high recovery of cellulose in required for further nanocellulose synthesis. Ionic liquid treatment is another green process that fit well into the cellulose isolation with high recovery of all bio-compounds, high thermal stability and low volatility. The effects towards hemicellulose and lignin are depending on the nature of ionic liquid used. However, using ionic liquid for biomass pretreatment is not economically friendly as it is expensive in cost.

In bleaching process two treatments, namely treatment with chlorine compounds (chlorine, chlorine oxide, sodium chlorite, sodium hypochlorite) under acidic condition (more effective), and treatment with hydrogen peroxide (H_2O_2) under alkaline condition are well known (Malucelli et al., 2017; Taflick et al., 2017). The acid chlorite treatment is widely used to remove most of lignin and other components by the combination of distilled water, sodium chlorite, and acetic acid stirring with lignocellulosic biomass at 70–80 ^{o}C for 4–12 h. The acetic acid and sodium chlorite are fed to the mixtures at interval time, i.e., at every hour, for controlling the pH value. After that, the mixture is kept stirring overnight,

followed by washing with distilled water until reaching the neutral pH. The obtained solid products are collected and dried in oven at 50 ^{o}C, which is defined as holocellulose, mainly including hemicellulose and cellulose in the fibers. The white color fiber of holocellulose indicates the successful removal of lignin and other impurities.

2.4.2.3.2 Acid hydrolysis

Acid hydrolysis is the most common method for the extraction of nanocellulose from cellulosic materials by dissolving amorphous domains of cellulose fiber and results in nanocrystalline cellulose. Due to the combination of ordered and disordered regions in cellulose chains, the disordered regions can be easily hydrolyzed by acid and the ordered parts are left as the remaining. Acid hydrolysis method is better due to various reasons such as (1) it presents lower cost and good efficiency to obtain nanocellulose; (2) it is easy and fast to produce nanocellulose that has a better property; (3) it gives nanocellulose with higher crystallinity index and smaller size than other methods. The recovery and reusage of concentrated acid also make it more economical and environmentally friendly. Some of the most important controlling parameters that affect the properties of obtained nanocellulose during acid hydrolysis process include reaction temperature, reaction time and acid concentration (Lee et al., 2016a). A long time of reaction is needed for acid treatment at a low temperature (25-30) ^{o}C. On the other hand, if the hydrolysis temperature is higher than 60°C darkening of cellulose particles takes place due to hydration and carbonization. Therefore, the optimal temperature of the acid treatment is in the range of 45–60°C. The nanocrystalline cellulose that is formed through the acid treatment is of colloidal dimensions and forms an aqueous suspension when stabilized. The critical concentration of colloidal suspension, which is the lowest concentration where the whiskers self-organize, depends on particle size, acid treatment, preparation condition, aspect ratio, and ionic strength.

Different acids that have been used for acid hydrolysis of lignocellulosic fibers includes: sulfuric acid (H_2SO_4), hydrochloric acid (HCl), phosphoric acid (H_3PO_4), hydrobromic acid (HBr), and nitric acid (HNO_3) (Bhat et al., 2017). It should be noted that the use of different acids may lead to different effects on crystalline nanocellulose. For instance, treatment with hydrochloric acid results in reduced dispersion of crystals, leading to their flocculation when in solution, lowest crystallinity index due to its higher tendency to

promote the breakage of the hydrogen bonds in the crystalline region of cellulose (Malucelli et al., 2017). H_2SO_4 is the most common acid used for acid hydrolysis process because it produces CNCs particles grafted with the negatively charged sulfate ester group which makes the CNCs particles a negative electrostatic repulsion force. The sulfate groups of H_2SO_4 may react with surface hydroxyl groups of cellulose, yielding charged surface esters that promote dispersion of nanocrystals as a stable colloid system in water (Abitbol et al., 2016; Lee et al., 2014; Wang et al., 2017). Therefore, hydrolysis with sulfuric acid is more advantageous. The washing process is usually performed by adding cold water followed by centrifugation until neutral pH is reached. The suspension was collected until it began to become turbid. The precipitate was diluted and centrifuged repeatedly in order to collect the turbid suspension maximally. The collection process was stopped until the suspension became clear again. The turbid suspension collected was subjected to dialysis against distilled water for several days until a constant pH was obtained. Finally, the suspension is dried with freeze dryer to get powder of nanocrystalline cellulose. The pretreatment methods, acid hydrolysis and the process conditions used by different studies to produce crystalline nanocellulose are summarized in Table 2.2.

Table 2.2. Summaries of some common literatures on process conditions

Lignocellulosic materials	Pretreatment methods chemical used		Acid-hydrolysis (chemical used and process conditions)	Reference
	Alkaline treatment (chemicals and process condition used)	Bleaching (chemicals and process condition used)		
Water Hyacinth Fiber	15 % NaOH in the ratio of 1:10(g/ml) at 130 ^{o}C for 6 h	Mixture of sodium chlorite and acetic acid with the ratio of 4:1 (v/v) at 60 ^{o}C for 2 h	5 M hydrochloric acid at 60 ^{o}C for 20 h under constant agitation and sonication	(Asrofi, Abral, Kasim, Pratoto, Mahardika, Park, et al., 2018)
Red algae waste	4wt% NaOH solution at 80 ◦C for 2 h under stirring	Aqueous sodium chlorite (1.7 wt% $NaClO_2$ in water) at 80 ^{o}C for 2 h	64 wt% H_2SO_4 at 50 ^{o}C for 30, 40 and 80 min.	(El et al., 2018)
waste cotton cloth	NaOH 10% (wt%) at 70 ^{o}C for 2 h	Hydrogen peroxide 1.5% (wt.%) under similar condition as alkaline treatment	Mixture of HCl, H_2SO_4, water at 55 ^{o}C for 7 h	(Wang et al., 2017)
Humulus japonicus stem	4% (Wt/V) NaOH at 80 ^{o}C for 2 h	5%acidifiedsodium chlorite (NaClO2+ CH3COOH, at 80 ^{o}C for 2 h	60% sulfuric acid at 45 ^{o}C for 1 h with strong agitation.	(Y. Jiang et al., 2017)
Corncob residue	3% (wt/wt) NaOH for 3 h at 100 ^{o}C	Sodium hypochlorite (0.02 g per gram of sample) at 80 ^{o}C for 2 h	64 wt% H_2SO_4 with a liquid-to-solid ratio of 20 ml/g at 45 ^{o}C for 60 min	(Liu et al., 2016)
Palm Oil Empty Fruit Bunch	2 % (wt/wt) NaOH for 3 h at 70 °C under constant stirring	acetate buffer with 1.7 % sodium chlorite at 80 °C for 2 h under agitation	64 % (wt/wt) H_2SO_4 at 40 °C for 45 min under strong agitation	(Shanmugarajah et al., 2015)
pineapple leaf	NaOH 2% (wt/wt) for 4 h at 100 ^{o}C under mechanical stirring	1.7 wt% $NaClO_2$ in water, mixtures of 27 g of NaOH and 75 ml glacial acetic acid in 1 L of distilled water at 80 ^{o}C for 4 h.	H_2SO_4 64%(wt/wt) at 45 ^{o}C for 5 min, 30 min or 60 min under constant stirring	(Santos et al., 2013)

Generally, these methods have been used in different studies to produce nanocellulose from various lignocellulosic biomasses. Figure 2.2 summarizes the general flow diagram for

processing lignocellulosic materials to nanocellulose and the comparison of these methods with respect to the dimension of obtained nanocellulose is given in Table 2.3.

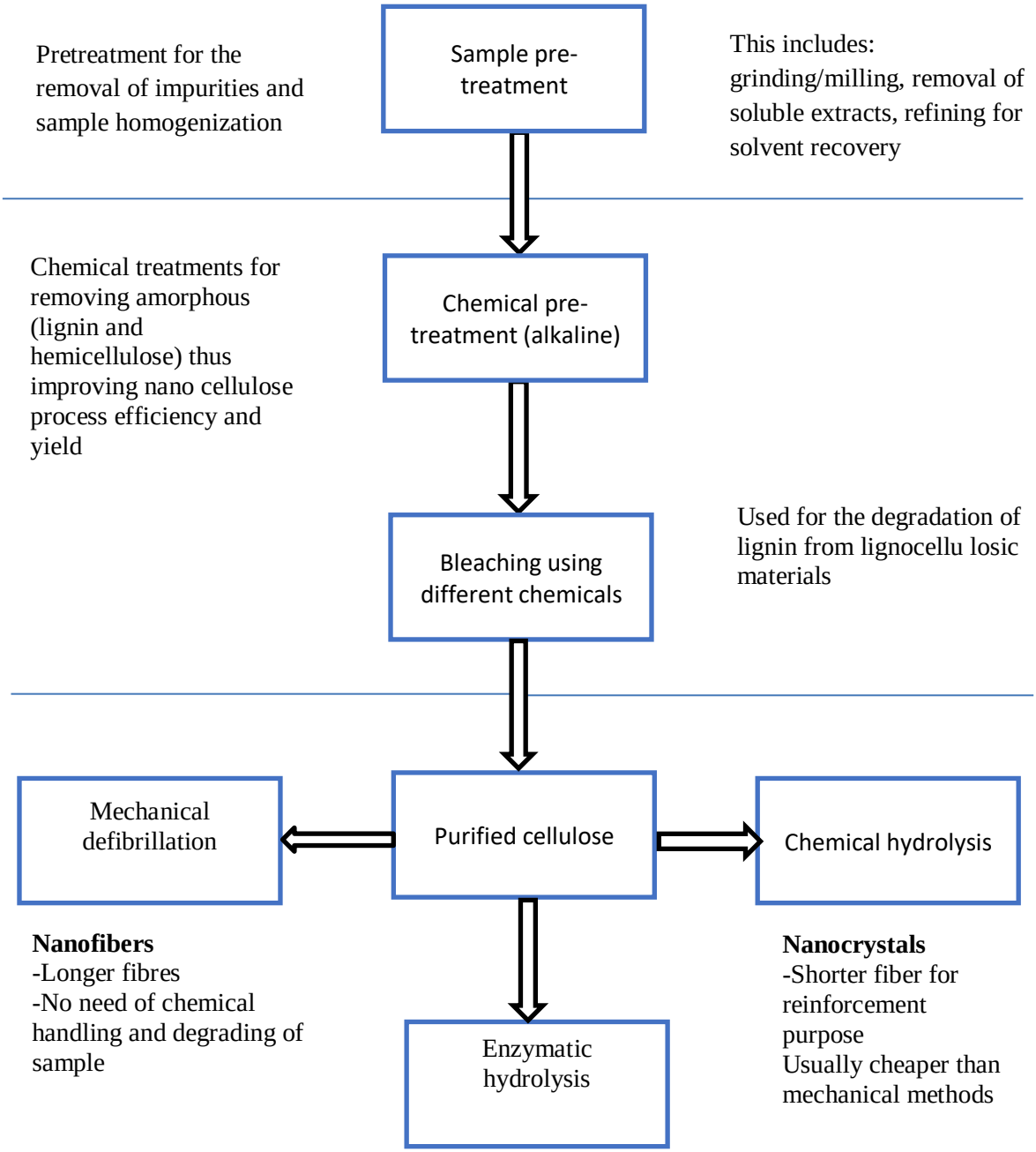

Figure 2.2. General procedures for processing of lignocellulosic materials to nanocellulose

(Malucelli et al., 2017)

Table 2.3. Comparison of nanocellulose preparation methods

Sources	Synthesis process	Size (length=L or diameter=D)	References
Red algae waste	Acid hydrolysis	L=248.5-321.5 nm D=2.1-7.9 nm	(El et al.,2018)
Agricultural waste corn stover	Mechanical (High-pressure homogenization)	-	(Xu et al., 2018)
Waste cotton clothe	Acid hydrolysis	(28- 470) nm in length, 3–35 nm in diameter	(Wang et al., 2017)
Humulus japonicus stem	Acid hydrolysis	6.13-16.35 nm of average diameter	(Y. Jiang et al., 2017)
Kenaf core	Electron-beam irradiation and acid hydrolysis	-	(Lee et al., 2016a)
Corncob residue	Acid hydrolysis and mechanical methods	L=140 nm, D= 5 nm	(Liu et al., 2016)
Arecanut husk fibre	Mechanical (Homogenization)	-	(George et al., 2016)
Garlic straw residues	Acid hydrolysis	L (480nm), D (6nm)	(Kallel et al., 2016)
Culinary banana peel	High-intensity ultrasonication combined with chemical treatment	D=24.7- 39.3 nm and L=462.57-475.17nm	(Xie et al., 2016)
Sugarcane bagasse	Acid hydrolysis	111-196.7 nm of average diameter	(WT Wulandari, 2016)
Lotus Leaf Stalk Agro-wastes	High-intensity ultrasonication with chemical treatment	D= 20 ± 5 nm and Length in micron scales	(Yandan et al., 2015)
Tomato peels	Acid hydrolysis	L=135±50 nm D=7.2 ±1.8 nm	(F. Jiang & Hsieh, 2015)
Citrus waste	Enzymatic hydrolysis	10 nm	(Mariño et al., 2015)
pineapple leaf	Acid hydrolysis	-	(Santos et al., 2013)

2.4.3 Properties of nanocellulose

Nanocellulose has attracted great attention due to their unique physical and chemical characteristics such as sustainability, biodegradability, low density (~1.566 g cm^{-3}), renewability of cellulose, highly abundant availability, high aspect ratio (L/D) 2-20, biocompatible, low energy consumption and low cost (Mashego, 2016). Additionally, the nanocellulose possesses a very large surface-to-volume ratio, better uniformity and durability, high crystallinity, high modulus of elasticity (~150 GPa), high tensile strength

(in the range of 7.5-7.7 GPa), high stiffness, flexibility, and good thermal, electrical, extremely absorbent and optical properties (Yahya et al., 2015). Because nanocellulose is highly crystallized through hydrogen bonding, its tensile strength is five-times higher than that of ferrous metal. In contrast, its coefficient of thermal expansion is less than one-tenth that of glass fiber (Lee et al., 2016a). Furthermore, the materials that are present in nanoscale range possess a different electronic property, which successively affects its optical, catalytic, and other reactive properties (Bhat et al., 2017; Lee et al., 2014; Missoum et al., 2013).

The stiffness, aspect ratios, and the ability to align under certain conditions make crystalline them ideal for exhibiting liquid crystalline behavior. The liquid crystallinity of nanocrystals coupled with the birefringent nature leads to interesting optical phenomena. The type of acid used for hydrolysis can affect the liquid crystalline nature. The CNCs obtained by sulfuric acid hydrolysis often possesses a negatively charged surface, which promotes uniform dispersion in water due to electrostatic repulsions. Even though the interactions between nanocrystals are strong, highly sulfonated CNCs is readily dispersible and this leads to the development of lyotropic behavior. Sulfuric acid and phosphoric acid-derived CNCs normally give chiral nematic structure, whereas hydrochloric acid derived CNCs with postreaction sulfonation give rise to a birefringent glassy phase. Properties such as liquid crystallinity, ordering, and gelation can influence rheological parameters of CNCs. Dilute CNCs suspensions show shear thinning behavior, which shows concentration dependence at low rates. At higher concentrations, in which the suspensions are lyotropic, they exhibit anomalous behavior. The main reason for such behavior is that the rod-shaped nanocrystals tend to align at a critical shear rate. As the shear rate reaches a critical point, the chirality of the CNCs suspension breaks down in favor of a simple nematic structure. In addition, the relaxation time constant depends on the aspect ratio, and CNCs with higher aspect ratios stay aligned for longer times even after shear. The type of acid used for hydrolysis can also influence the rheological properties of CNCs suspensions. Sulfuric acid treated crystals show some shear thinning that is independent of time, while HCl- derived crystals show much higher shear thinning behavior (George & S N, 2015).

2.4.4 Application of CNCs

Currently, CNCs is a suitable nanomaterial for a wide range of application in different fields such as the automotive and construction industries, electronic components, enzyme immobilization, synthesis of antimicrobial, sports and leisure, packaging materials, green catalysis, biosensing, paper production, polymer nanocomposites and biomedical application (George & S N, 2015; Herrera Rodriguez, 2015; Malucelli et al., 2017; Mashego, 2016; Mishra et al., 2018; Xie et al., 2016). Nanocrystalline cellulose can also be used to make aerogels and foams for packaging application as an alternative to polystyrene-based foams. Generally, the utilization of CNCs for various applications can be of two broad types: one type involves the use of functionalized or non-functionalized as synthesized CNCs, and the other one involves the use of polymer nanocomposites wherein CNCs acts as a reinforcing agent.

2.4.4.1 Medical, cosmetic and pharmaceutical

The versatility and adaptability of this material enables nanocrystalline cellulose to be utilized for biomedical applications. Given that one of the characteristics of medical biomaterials is biocompatibility, or the ability to function properly in the human body to produce the desired clinical outcome without causing adverse effect, nanocrystalline cellulose as a bio-derived material can be a promising biomaterial (Malucelli et al., 2017). Nanocrystalline cellulose as drug delivery excipients is due to its properties such as smaller size, hydrophilicity and biocompatibility (Abitbol et al., 2016). Large quantities of drugs can be bound to the surface of CNCs with the potential for optimal control of dosing due to its properties such as large surface area and possibility of acquiring negative charge during hydrolysis. The abundant surface hydroxyl groups present in nanocrystals provide sites for surface modification with a range of chemical groups. Surface modification can be used to modulate the loading and release of drugs that do not normally bind to cellulose, such as nonionized or hydrophobic drugs. Due to their open pore structure and high surface area, which can provide enhanced drug bio-availability and better drug-loading capacity, CNCs-based aerogels are also receiving growing interest in biomedical and pharmaceutical applications (Malucelli et al., 2017). The use of nanocellulose in cosmetics and pharmaceuticals was also early recognized. A wide range of high-end applications have been suggested as: freeze-dried nanocellulose aerogels used in sanitary napkins, tampons,

diapers or as wound dressing; nanocellulose used as a composite coating agent in cosmetics (e.g. for hair, eyelashes, eyebrows or nails); a dry solid nanocellulose composition in the form of tablets for treating intestinal disorders; nanocellulose films for screening of biological compounds and nucleic acids encoding a biological compound; filter medium partly based on nanocellulose for leukocyte free blood transfusion; powdered nanocellulose has also been suggested as an excipient or bulking agent in pharmaceutical compositions (Abitbol et al., 2016). An excipient is a natural or synthetic substance formulated alongside the active ingredient of a medication, included for the purpose of bulking-up formulations that contain potent active ingredients; nanocellulose in compositions of a photo reactive noxious substance purging agent; elastic cryo-structured gels for potential biomedical and biotechnological application.

2.4.4.2 CNCs as nanocomposite to improve properties of polymers

Research has pointed out that cellulose based materials employed in the composite system provide excellent physical as well as chemical features together with environmentally friendly capabilities. Polymer nanocomposite is the term for a multiphase material wherein the polymer phase matrix having filler or reinforcement in at least one dimension in the nanometer range. Fundamentally, it is nicely described that the attributes of nanocomposite are decided by uniform distribution and dispersion of nanofillers in polymer matrices as well as the interaction established between them (Malucelli et al., 2017; Mishra et al., 2018). These polymer nanocomposites exhibit unique properties because of their nanometric size and the increased surface area of the reinforcing material. The high strength and stiffness as well as the small dimensions of nanocrystalline cellulose may well impart useful properties to composite materials reinforced with these fibers, which could subsequently be used in wide range of applications (Bhat et al., 2017). Bio-composites consisting of the polymer matrix and natural cellulose fibres are environmentally-friendly materials which can replace glass fibre-reinforced polymer composites. The polymer properties such mechanical, ionic conductivity and thermal properties can be improved by using nanocrystalline cellulose as nanocomposite material in polymer processing. Nanocrystalline cellulose is used as the load bearing constituent in many polymer nanocomposite systems as it can produce significant improvements in mechanical properties even at very low volume fractions. Furthermore, its high aspect ratio, good

dispersion in hydrophilic systems and the capability to form percolated network type architecture within the polymer matrix make it a widely preferred reinforcing component. In the area of polymer nanocomposites, CNCs are also used as model nanofillers with a defined morphology to impart sufficient strength and modulus. Good dispersibility of the CNCs in the polymer matrix is a prerequisite to make polymer nanocomposites with better properties, as a nonhomogeneous dispersion of the filler in the polymer matrix decreases the final mechanical properties of the nanocomposite material. CNCs can form stable colloidal dispersions in water and hence they are best suited for water-soluble or water-dispersible polymers such as latexes.

2.4.4.3 Paper and paperboard

CNCs have also potential application in the paper and paperboard industry where they can increase the fibre-fibre bond strength and thereby increasing the strength of the paper. CNCs can also be used as a barrier in grease- proof type of papers and as a wet-end additive to enhance retention, dry and wet strength in commodity type of paper and board products (Mashego, 2016)

2.4.4.4 Food

As a food thickener, CNCs can be used as a low-calorie replacement for carbohydrate additives, as a flavour carrier and suspension stabilizers. It can also be used to produce fillings, crushes, chips, wafers, soups, gravies, puddings as well as oxygen barriers for food packaging (Yahya et al., 2015). The food applications of CNCs were one of the earliest applications of nanocellulose due to the rheological behavior of the nanocellulose gel.

2.4.4.5 Hygiene and absorbent products

In this field, CNCs has different applications such as: super water absorbent (e.g. material for incontinence pads material); nanocellulose used together with super absorbent polymers; nanocellulose in tissue, non-woven products or absorbent structures and also as antimicrobial films (Malucelli et al., 2017).

3. Materials and Methods

3.1 Materials

3.1.1 Equipment and Instruments

The equipment and instruments such as miller, soxhlet apparatus, pH meter, autoclave reactor, oven, tray dryer, desiccator, centrifuge, refrigerator, dialysis membrane, ultrasonicater, vacuum rotary evaporator and freeze dryer were used in this study. Furthermore, instruments such as Particle Size Analyzer (ZEN3600), Scanning Electron Microscopy (FEI-INSPECT-F50), Attenuated Total Reflection Fourier Transform Infrared Spectroscopy (Thermo SCIENTIFIC iS50 ABX), and X-ray diffraction (BTX-528) were used for characterization of the samples.

3.1.2 Chemicals and Reagents

The reagents and chemicals used in this study were toluene (99%), ethanol (97%), sodium hydroxide (97%), sodium hypochlorite, distilled water, acetic acid (99.5%), sulfuric acid (95%), and chloroform (99%). All the chemicals used in experiments were of analytical grade.

3.2 Methods

3.2.1 Isolation of Cellulose

Water hyacinth was collected from Koka dam by mechanical means. To isolate and purify cellulose from water hyacinth, the raw sample was passed through different pretreatment steps. The basic pretreatments such as size reduction, extraction of soluble components, alkaline treatment and bleaching were performed in this study for the removal of impurities and sample homogenization.

3.2.1.1 Size reduction and extraction of extractive components

First, the stems of mechanically collected water hyacinth were separated from its leaves and roots using laboratory knife. Next, the collected stems were washed with distilled water to remove dusts and then dried in an oven at the temperature of 60 ^{o}C for 24 h. The dried sample was chopped, milled and sieved using 60-mesh (250 µm) sieve to get the powder form of sample (Jiang & Hsieh, 2015; Lu & Hsieh, 2012). Next, the obtained powder was sealed in plastic (polyethylene) bag and stored in desiccator until use. The sample was dewaxed in a soxhlet apparatus using mixture of toluene and ethanol solvents with the ratio of 2:1 (v/v) (F. Jiang & Hsieh, 2015; Ching et al., 2016). The de-waxing process was

conducted at 85 ^{o}C for 5 h to remove extractive components such as wax, pectin and oils. The de-waxed powder was washed with distilled water and ethanol repeatedly; filtered using 45 µm sieve to remove solvents and finally dried in oven at 45 ^{o}C.

3.2.1.2 Alkaline Pretreatment

This step was used to reduce amorphous content (lignin and hemicellulose) and to improve nanocellulose production process efficiency and yield. The dewaxed sample was treated twice in autoclave reactor (HPA-1L) with 4 % (wt /wt) NaOH solutions at 80 ^{o}C for 2 h under constant agitation at 500 rpm. The ratio of dewaxed sample to NaOH solution used for alkaline treatment was 1:20 (g/ml) (Lee et al., 2014). The treated sample was repeatedly washed after each treatment using diluted acetic acid and distilled water to neutral pH. Successive centrifugation at 4000 rpm was also performed during washing to separate the sample from solvent. Then, the sediment obtained from centrifugation was dried in tray drier (TDC/EV) at 45 ^{o}C to constant weight and the size reduction was done for next treatment since it can compact during drying.

3.2.1.3 Bleaching

After alkaline treatment, the dried sample was bleached using a mixture of 6% (wt/wt) sodium hypochlorite solutions and acetic acid with the ratio of 4:1 (v/v) under acidic condition at pH of 4 (D.-Y. Kim et al., 2016). The ratio of sample to solvent used was 1:20 (g/ml). The process was performed twice in autoclave reactor at 80 ^{o}C for 2 h under constant agitation at 500 rpm again to remove lignin (Abraham et al., 2011). The bleached sample was cooled in reactor by using chiller connected with reactor. Then, it was washed repeatedly with diluted solution of sodium hydroxide and distilled water until free from acid and to achieve neutral pH. During washing step, the successive centrifugation was performed by replacing supernatant with distilled water until white cellulose was obtained. Finally, the obtained white cellulose was frozen using deep freezer and then freeze dried to obtain powder cellulose. The cellulose powder obtained from freeze drier was sealed in plastic bag and stored in desiccator until use or characterized.

3.2.2 Preparation of cellulose nanocrystals

A controlled H_2SO_4 hydrolysis was performed in autoclave reactor to split the amorphous domains, remove local interfibril crystalline contacts of the pretreated sample. The three most important parameters selected were reaction temperature, reaction time and acid

concentration. Purified cellulose was acid hydrolyzed using 10g of cellulose in 250 ml of sulfuric acid for one run (1g: 25ml) under controlled conditions and continuous agitation at 500 rpm (Wulandari et al., 2016). Three levels of acid concentrations (50 %, 57.5 % and 65 %), temperature (40 ^{o}C, 50 ^{o}C, and 60 ^{o}C) and reaction time (30 min, 45 min and 60 min) were used based on literatures and experimental design from Response Surface Method (RSM) (Wang et al., 2017). The hydrolysis reaction was quenched by adding ice to autoclave reactor. The hydrolyzed cellulose sample was then washed repeatedly with successive centrifugation at 4000 rpm for 25 min to remove excess sulfuric acids (Ghazy et al., 2016). The suspension was collected and diluted with distilled water. The suspension was then dialyzed against deionized water using cellulose membrane for 4 days to neutralize and fully remove free acid molecules such as non-reactive sulfate group, salts as well as soluble sugars. After dialysis, the obtained suspension of CNCs was ultrasonicated for 15 min to get aqueous homogenized dispersion and labeled as the CNCs suspension (Marimuthu & Atmakuru, 2015). Then, a few drops of chloroform were added to the freshly prepared suspension to prevent degradation of the cellulose nanocrystals and then stored in refrigerator at 4 ^{o}C for characterization. Finally, the cellulose nanocrystals suspension was freeze dried to obtain CNCs in powder form for some characterization and the yield of dried CNCs was calculated as shown below:

$$Yield\ of\ CNCs\ (Y\ \%) = \frac{W1}{W2} \times 100 \ldots\ldots\ldots\ldots\ldots\ldots\ldots 3.1$$

where, Y represents yield, W_1 represents dried weight of cellulose after hydrolysis and W_2 represents dried weight of CNCs obtained before hydrolysis. Generally, the overall steps performed to extract CNCs and the results obtained at each step were summarized by the flow diagram shown in Figure 3.1.

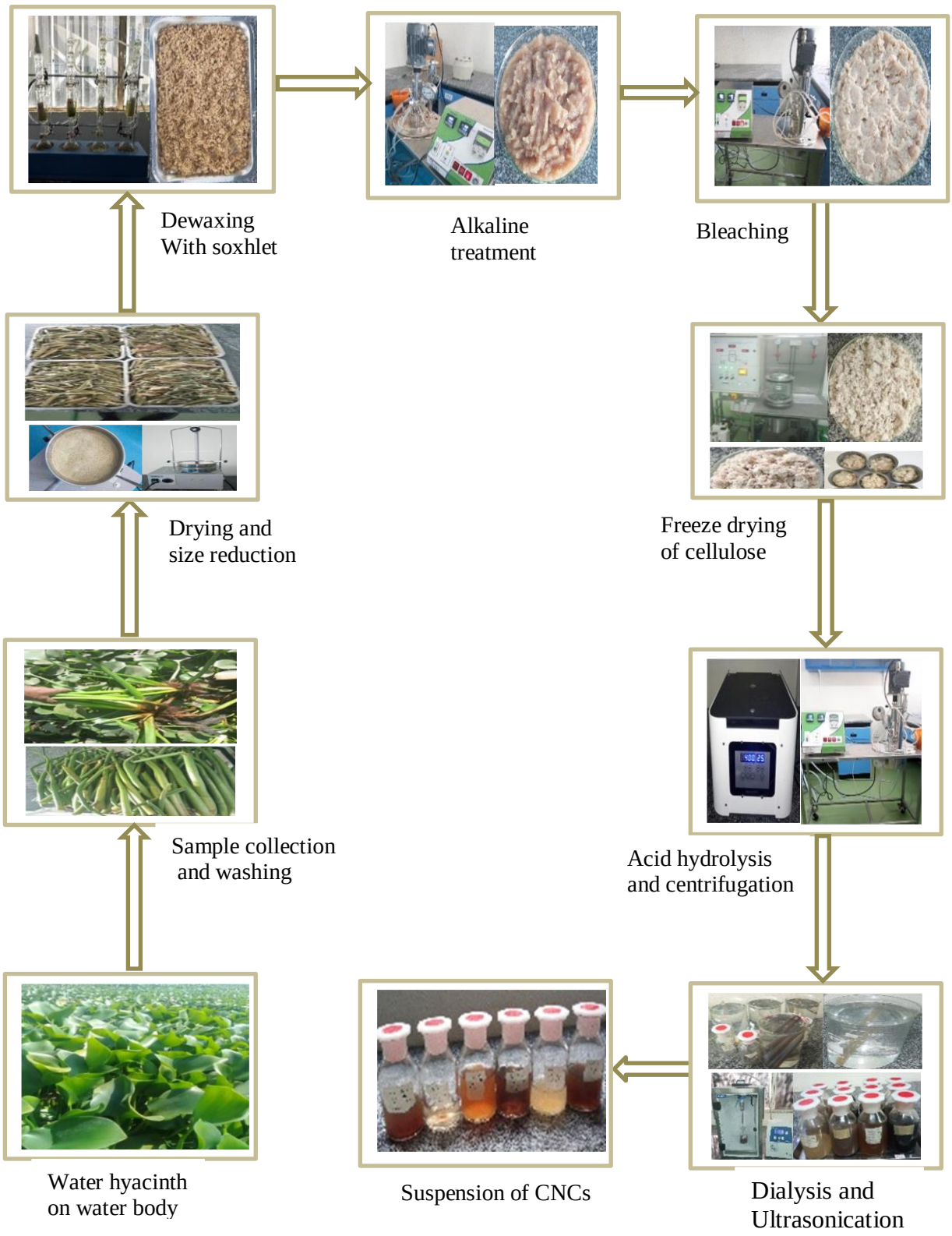

Figure 3.1. Flow diagram for the production of CNCs from water hyacinth

3.3 Experimental Design for Response Surface Method (RSM)

RSM is a collection of statistical and mathematical methods that are useful for the modeling and analyzing engineering problems. Optimizing the response surface that is influenced by various process parameters and quantifying the relationship between the controllable input parameters and the obtained response surfaces are the main objectives of the RSM. It also allows us to estimate interaction and even quadratic effects, and therefore give us an idea of the local shape of the response surface under investigation. Box-Behnken designs and central composite designs are efficient designs for fitting second order polynomials to response surfaces, because they use relatively small number of observations to estimate the parameters and provides equal precision of estimation in all directions (Ranganath, 2015). Rotatability is also a reasonable basis for the selection of a response surface design.

A box-Behnken design (BBD) is nearly rotatable and having the maximum efficiency for an RSM problem involving three factors and three levels. Also, the number of runs required is less compared to a central composite design (Stamenkov et al., 2018). Therefore, the experiments were planned and conducted according to a Box-Behnken type response surface design using three levels for each process parameters (Ranganath, 2015). Reaction temperature, reaction time and acid concentration were selected as the process parameters and optimized to ensure their effect on the response of the work. Each factor consisted of three levels such that temperature (40, 50, 60) ^{o}C, time (30, 45, 60) min and acid concentration (50, 57.5, 65) %. Based on the number of factors and level required, 15 total runs were conducted for BBD for modeling a response surface. Details of the experimental runs with the set of input parameters that were conducted are given in Table 3.1 with parameters corresponding to the central point repeated twice to establish that the experimental data within the normal dispersion and repeatability is ensured. Analysis of variance (ANOVA) was used to check the adequacy of the model for the responses in the experimentation. It is a statistical decision-making tool used for detecting any differences in average performances of tested parameters. It employs sum of squares and F statistics to find out relative importance of the analyzed processing parameters, measurement errors and uncontrolled parameters.

Table 3.1. Experimental design matrix for Box-Behnken designs.

Std	Run	Factors		
		A: Temper-ature, ^{o}C	B: Time, min	C: Acid concen-tration, %
11	1	50	30	65
13	2	50	45	57.5
8	3	60	45	65
2	4	60	30	57.5
12	5	50	60	65
6	6	60	45	50
14	7	50	45	57.5
7	8	40	45	65
4	9	60	60	57.5
1	10	40	30	57.5
5	11	40	45	50
10	12	50	60	50
15	13	50	45	57.5
3	14	40	60	57.5
9	15	50	30	50

3.4 Characterization of cellulose nanocrystalline

3.4.1 Particle Size Determination

Particle size distribution of obtained cellulose nanocrystals was measured using Malvern Zetasizer nano (ZE3600) to indicate the extent of the hydrolysis reaction. CNCs suspension was diluted with distilled water and the measurement was conducted at 25 ^{o}C with a calibration time of 80 seconds. The particle size is determined by measuring the random changes in the intensity of light scattered from a suspension. The obtained data was then processed by using Malvern Zetasizer software.

3.4.2 Fourier Transform Infrared Spectroscopy

Attenuated Total Reflection Fourier Transform Infrared Spectrometer (ATR-FTIR) was used for studying the change of the functional groups of the materials before and after their production process. Dried powder of WH, bleached cellulose and CNCs samples were tested and the spectra of the samples were recorded over an average of 250 scans in the range of 4000 to 400 cm^{-1} wave number with 32 resolutions.

3.4.3 Scanning Electron Microscopy Studies (SEM)

SEM (FEI INSPECT F50 model) was used to produce the images of WH, bleached cellulose and CNCs samples by scanning the surface with a focused beam of electrons. The electrons interact with atoms in the samples, producing various signals that contain information about the surface morphology of the sample. This operation was done under vacuum at an accelerating voltage of 2 kV and x8984 magnification.

3.4.4 X-ray diffraction

The change in crystallinity index and crystal thickness of the samples from raw material to cellulose nanocrystals was evaluated by X-ray diffraction patterns. The powder of WH, bleached cellulose and CNCs samples were scanned at room temperature with diffraction angle in the range of 5^o to 80^o and a step size of 0.03^o. Then the crystallinity index of the analyzed samples was calculated through the empirical Segal's equation at scanning rate of 0.5^o/min.

$$Crystallinity, CI\ (\%) = \frac{I200 - Iam}{I200} \times 100 \ldots\ldots\ldots\ldots\ldots \quad 3.2$$

In this equation, I_{200} represents the maximum diffraction intensity values of crystalline at a 2θ ranged from 52.5^o to 57.5^o cellulose and I_{am} shows minimum intensity value of amorphous cellulose at 2θ ranged from 37.5^o to 40^o. Similarly, the crystal thickness (D) measured using Derby Scherer's equation at a given d-spacing (Shanmugarajah et al., 2015).

$$Crystal\ thickness\ (D) = \frac{k\lambda}{\beta cos\theta} \ldots\ldots\ldots\ldots\ldots\ldots\ldots\ldots \quad 3.3$$

Where k is for factor with value of 0.9, β represents full width half maximum of maximum intensity in radians and λ is a constant radiation with the value of 0.1574 nm.

3.4.5 Differential Scanning Calorimetry (DSC)

DSC analysis were performed to see thermal behavior of raw water hyacinth, bleached cellulose and CNCs samples. During measurement, 4 mg of each samples were placed in platinum crucible and heated from room temperature to 400 ^{o}C for 40 min at heating rate of 10 ^{o}C/min.

4. Result and Discussion

4.1 Isolation of Cellulose from water hyacinth

Cellulose was isolated from water hyacinth stem following different physiochemical treatment steps such as soxhlet extraction, alkaline treatment and bleaching. Extractive substances such as fats, waxes, alkaloids, proteins, simple and complex phenolic, simple sugars, pectins, starch, essential oils and other organic soluble ingredients were removed using soxhlet extraction. For this purpose, a mixture of toluene and ethanol with a ratio of 2:1 (v/v) was used as a solvent. After each pretreatment process, the green color of water hyacinth powder reduced and became pure white cellulose which was shown in Figure 4.1.

Figure 4.1. Bleached and freeze-dried cellulose

4.2 Nanocrystalline cellulose

After bleaching, the purified cellulose fibers were then subjected to a sulfuric acid hydrolysis in which CNCs was isolated showing high stability in water. The hydrolysis process was conducted at different hydrolysis time (30, 45 and 60 min), temperature (40, 50 and 60 ^{o}C) and with different acid concentration of (50, 57.5 and 65%). After hydrolysis, different steps such as successive centrifugation, dialysis, ultrasonication and freeze drying were performed to get purified CNCs. The yield of the CNCs obtained was varied depending on parameter interaction from experimental design. Figure 4.2 shows the obtained suspension of cellulose nanocrystals.

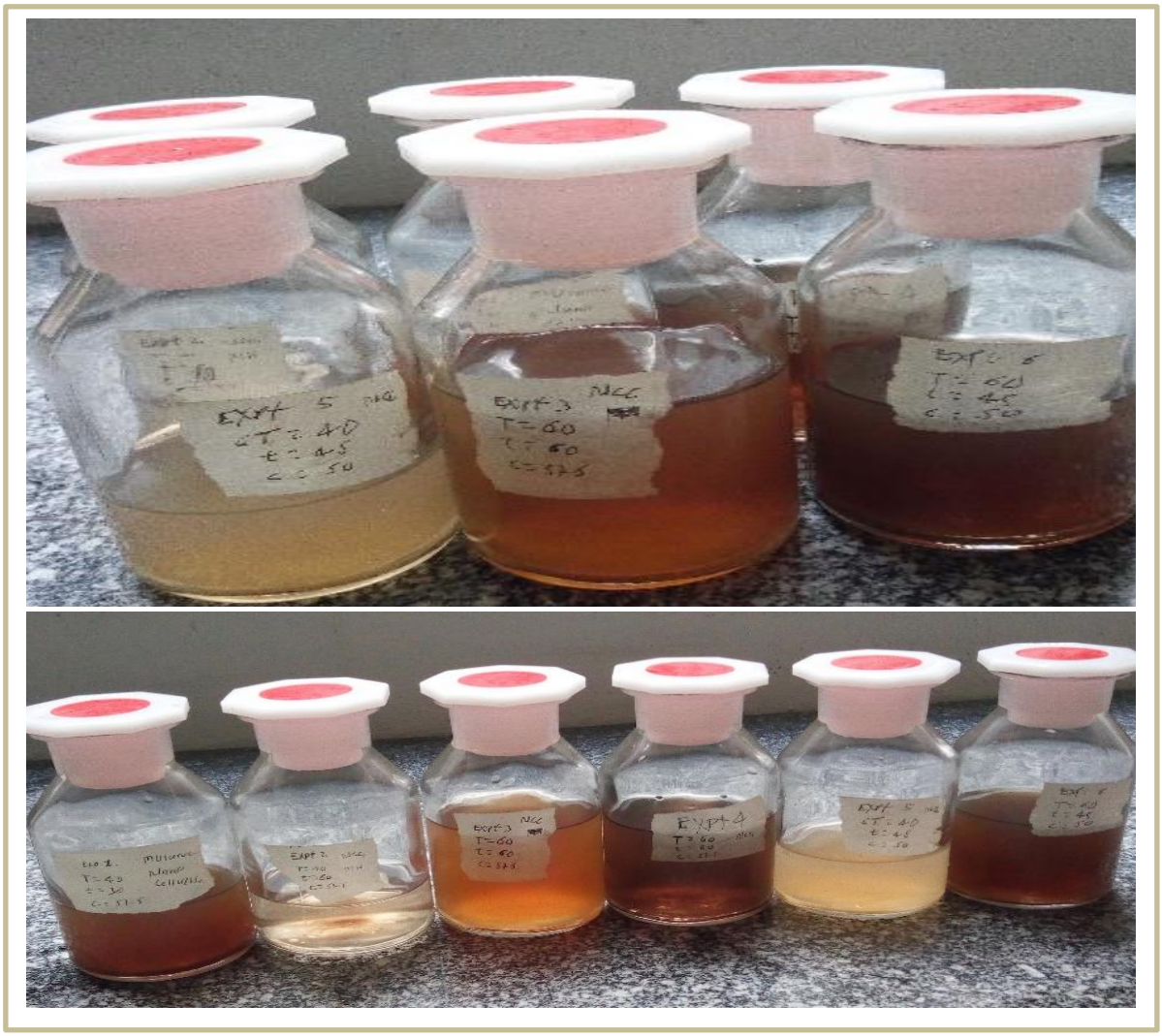

Figure 4.2. Suspension of crystalline nanocellulose after ultrasonication

4.3 Characterization

4.3.1 Morphological Analysis

The morphology of water hyacinth (WH), bleached cellulose and CNCs obtained were examined by SEM analysis as shown in Figure 4.3. From the image of SEM analysis, it is clearly shown that the extracted CNCs have a whisker-shaped structure which confirms its extraction from WH (Asrofi et al., 2018; Lee et al., 2016a) The obtained result also demonstrates the efficiency of the conditions used during acid hydrolysis and confirms that CNCs aqueous suspensions contained individual nanocrystals. From these images, it is also observed that the chemical treatment affects the morphological structure of the fibers with respect to surface smoothness and size.

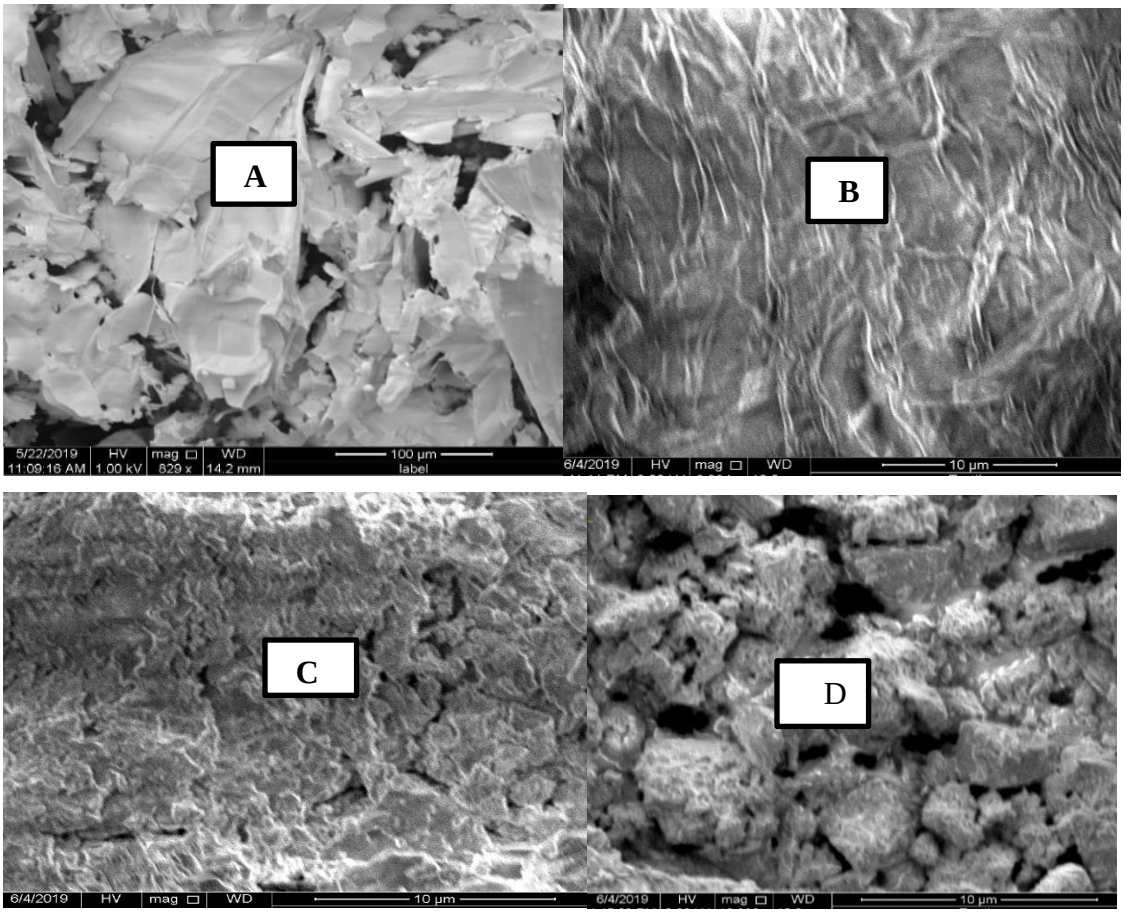

Figure 4.3. SEM Image of (A) raw water hyacinth, (B) cellulose after bleaching and (C, D) CNCs

The surface of water hyacinth fiber was smooth before chemical treatments and became rougher after chemical treatments. This shows the breaking of binding bonds formed by hemicellulose and lignin in natural fiber.

4.3.2 Fourier transform-infrared radiation analysis

FTIR analysis of WH, bleached cellulose and selected CNCs samples are shown in Figure 4.4. The ATR-FTIR (Thermo Scientific iS50 ABX) was used to characterize the chemical structure by identifying the functional groups present in each sample. The spectra of the samples were scanned over the wavelength from 4000 cm^{-1} to 400 $cm^{-1}$with 250 number of scans and at 32 resolution. In the spectrum of water hyacinth and CNCs, there were the peaks appeared at around 3734 cm^{-1} and 3614 cm^{-1} due to the presence of free O-H stretching sharp peak vibration (El Achaby et al., 2018). This OH group attributed to adsorbed water and aliphatic alcohols that can found in hemicellulose, cellulose and other extractive components. The peak at 1032 cm^{-1} is appeared due to C-O stretch which can provide information about alcohol structure in raw sample. The intensity of this peak was gradually increased from raw WH to CNC, indicating that the cellulose content was increased during different chemical treatments. The FTIR spectrum of WH shows a characteristic peak at 1527.86 cm^{-1} and 2346.92 cm^{-1} which are associated with the stretching vibration of N-H band of the protein amide structure as well as N-O stretching of nitro compounds and O=C=O stretching of carbon dioxide respectively (Lee et al., 2016b). The observed peaks at around 1032 cm^{-1} and 1034 cm^{-1} are associated with the presence of strong S=O stretching sulfoxide groups in raw water hyacinth and CNCs due to acid hydrolysis. The peaks found at 2285.43 cm^{-1} and 2187.14 cm^{-1} in the case of cellulose indicates the presence of weak C≡N stretching of nitrile and weak C≡C stretching of alkyne group respectively (Liu et al., 2016). Similarly, the peak appeared at around 2000 cm^{-1} for cellulose sample shows the presence of triple bond groups such as weak H-C bending as well as C=C=C stretching of aromatic compounds (El et al., 2018; Ching et al, 2016).

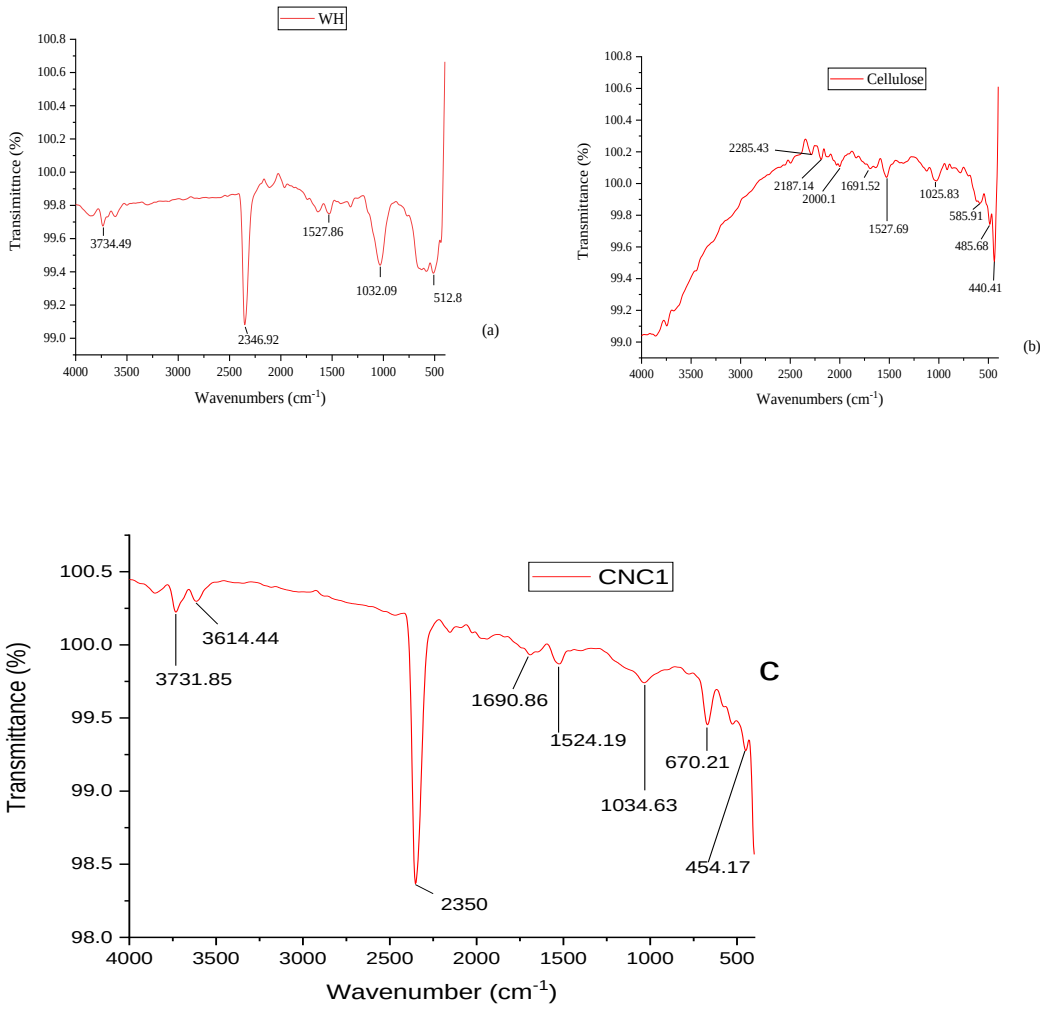

Figure 4.4. FTIR spectra of (a) raw water hyacinth, (b) bleached cellulose and (c) CNCs

The spectra appeared in the range of 3000 to 2850 cm^{-1} due to C-H stretching for alkenes and aromatics (Liu et al., 2016). The peaks appeared in the range of 1300 to 1000 cm^{-1} indicates the presence of ester with strong absorption due to the C-O bands. In CNCs sample the peaks found at 1690.86 and 1524.63 cm^{-1} indicates the presence of C=O stretching of conjugated aldehydes and strong N-O stretching of nitro compounds respectively (Lee et al., 2016b). There is also one peak appeared at around 670 cm^{-1} which shows the presence of strong C=C bending of alkene in CNCs sample.

4.3.3 X-ray diffraction (XRD) analysis

The crystalline structure and crystallinity index of WH, bleached cellulose and CNCs samples were analyzed by X-ray diffraction (BTX-528 model) as shown in Figure 4.5. Along with small shift in peak position, the XRD profiles for samples are similar indicating

that all samples contain cellulose. However, it is observed that there was a change in the relative intensity of the amorphous peaks and its width indicating a change in the crystallinity. The diffraction peak for raw water hyacinth was relatively broader and became sharper and narrower after chemical treatments. This indicates that the content of cellulose and degree of crystallinity was increased by chemical treatments.

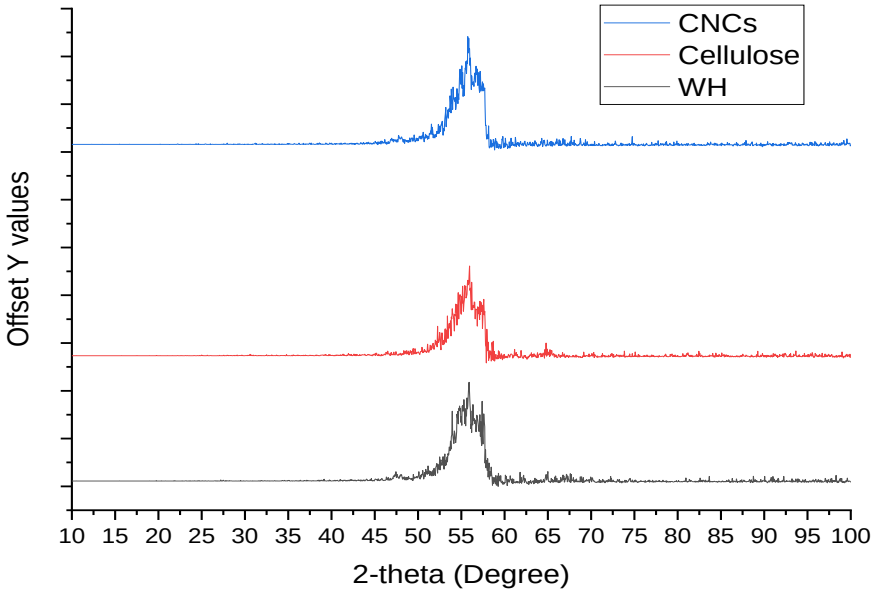

Figure 4.5. X-ray diffraction patterns of raw water hyacinth, bleached cellulose and CNCs The crystallinity index and crystal thickness of WH, bleached cellulose and CNCs samples were determined from Segal's and Scherer's equation (Lee et al., 2016b) and given in Table 4.1. From this result, it can be observed that the crystallinity index and crystal thickness of the analysed samples was improved through chemical treatments due to removal of non-cellulosic components and amorphous part of obtained cellulose

Table 4.1. Crystallinity index and crystal thickness at different treatment stages

Samples	Crystallinity index (%)	Crystal thickness (nm)	d-spacing (nm)
Water hyacinth	18	0.016	0.1034
Bleached cellulose	59	0.115	0.1427
CNCs	78	0.178	0.1789

4.3.4 Particle size analysis

Particle size analysis was done using Malvern Zetasizer nano (ZE3600) to determine the mean average of size. The measurement was conducted at room temperature and the particle size distribution of CNCs was obtained from diffusion light scattering (DLS) techniques. Figure 4.6 shows the particle size distribution for CNCs indicating an average particle size (diameter) of 102.6 nm at measurement position 4.65 and count rate of 328.2 (kcps).

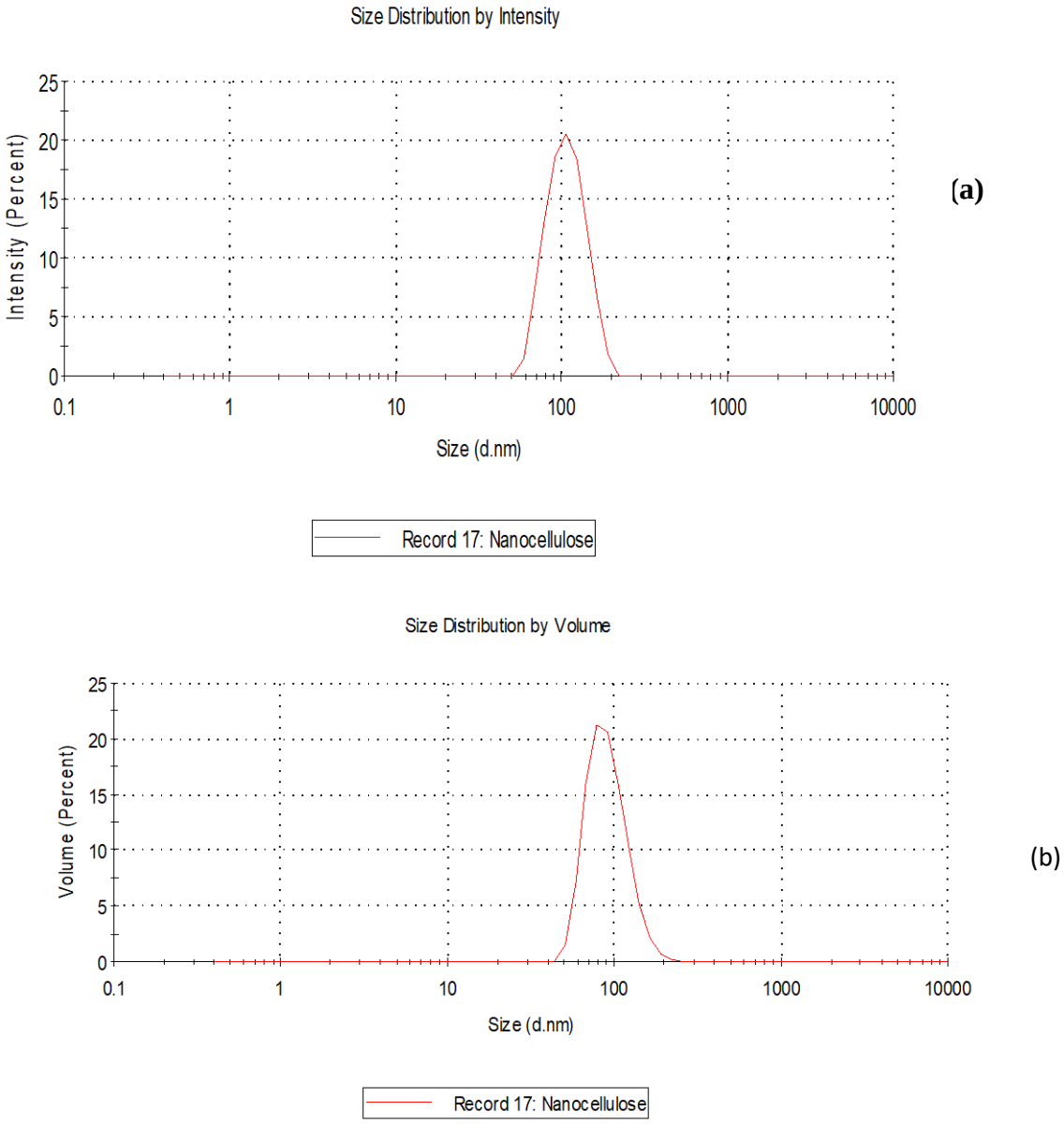

Figure 4.6. Particle size distribution by intensity and volume

During measurement, glass cuvette with round aperture was used as cell and thermal equilibration time taken was 80 second. It was observed that one major peak was recorded with average particle size of 102.6 at 100% intensity. As shown from Figure 4.6 (a) and (b), the size distribution of CNCs particles was ranged from 50.75 nm to 190.1 nm in diameter. Size distribution by volume data shows that CNCs particle with smaller size of 50.75 nm accountable for 1.5 % of volume while the particle with larger diameter of 190.1 nm accountable for 1.8 % volume. The CNCs particles with average diameter of 102.6 nm accountable for around 19 % of volume fraction.

4.3.5 Differential Scanning Calorimetry (DSC)

The thermal behavior of raw WH, bleached cellulose and CNCs were analyzed using differential scanning calorimeter (SKZ1052B). Figure 4.7 shows the thermograms of DSC for analyzed samples. As shown from Figure, an endothermic peak was present in all thermograms at temperature range from 25 ^{o}C to 100 ^{o}C due to water loss by evaporation (Nascimento, Marim, Carvalho, & Mali, 2016). Other endothermic peaks observed on the thermogram indicates the melting point and decomposition of the samples.

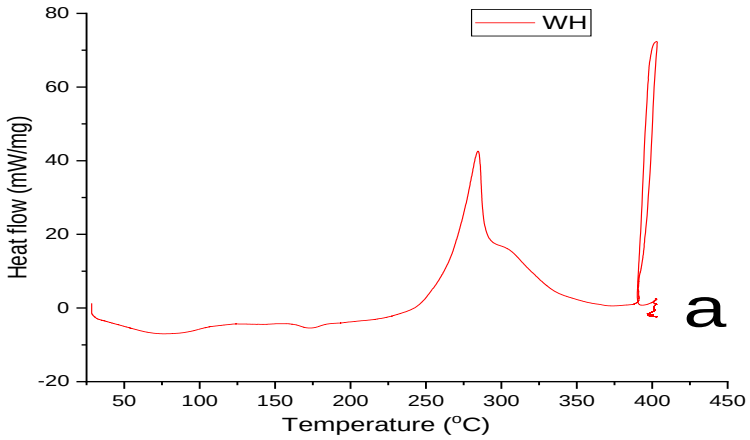

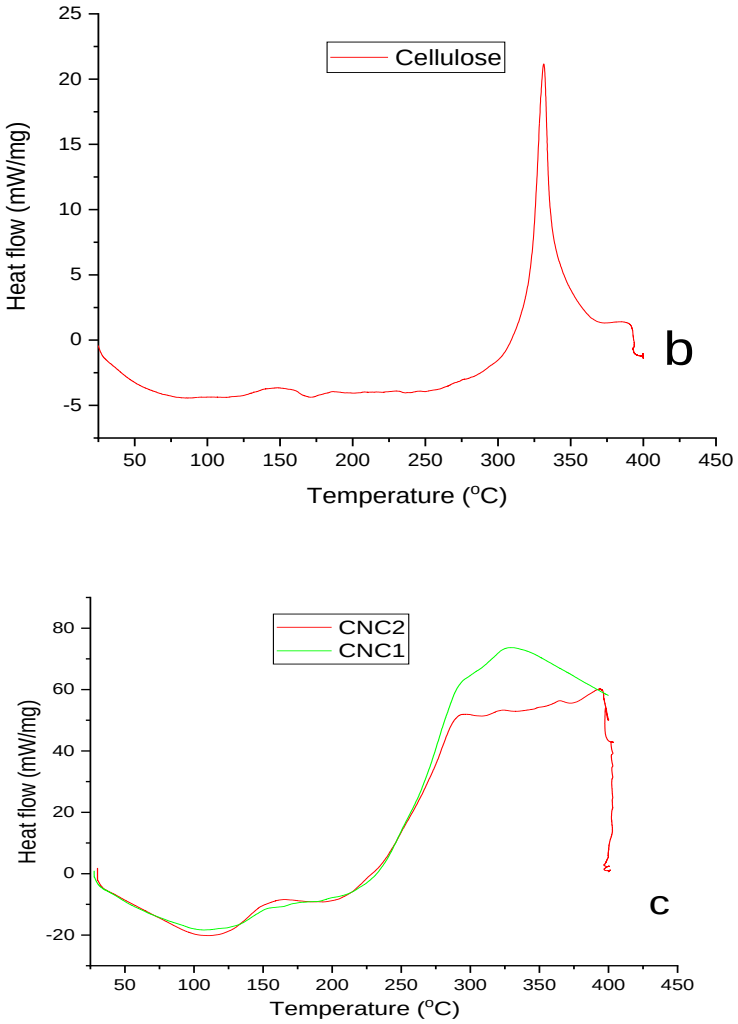

Figure 4.7. DSC thermograms for WH, bleached cellulose and CNCs

From the thermogram shown in Figure 4.7, it is observed that the position of the peaks increased after chemical treatment and higher for CNCs. This indicates that the amorphous part was decreased and the cellulose crystallite enhanced by chemical treatment. It is also observed that water hyacinth has a glass transition point at around 115 °C to 150 °C and for cellulose it was occurred at around 145 °C to 175 °C (Nascimento et al., 2016). The exothermic peaks found in all thermogram curves shows the decomposition point of the samples. Water hyacinth degraded at around 175 °C which is lower than that of cellulose and CNCs. This indicates the presence of impurities in raw material and removed after chemical treatment. Cellulose decomposed at around 325 °C implying the removal of impurities and for CNCs it was occurred at temperature range of 350 °C to 390 °C.

Generally, the result obtained from thermogram of DSC confirms that CNCs has high thermal stability and it been affected by chemical treatments (D.-Y. Kim et al., 2016; Wang et al., 2017).

4.4 Response Surface Methodology (RSM) Analysis

RSM is a collection of mathematical and statistical techniques that are useful for modeling and analysis in applications where several variables affect a response of interest. It is used in such a way that: it determines the factor levels that will simultaneously satisfy a set of desired specification; determine the optimum combination of factors that yield a desired response and describes the response near the optimum; determine how a specific response is affected by changes in the level of the factors over the specified levels of interest and find conditions for process stability. Therefore, it is considered as an appropriate approach to optimize a process with one or more responses. The relationship between the factors and the performance measures are expressed by multiple regression equations, which can be used to estimate the expected values of the performance level for any factor levels. For this study, a second-order model is utilized to find a suitable approximation for the functional relationship between independent variables and the response surface. Fifteen experiments were performed according to the BBD. The experimental conditions with their experimental and predicted responses with different combinations of parameters such as temperature, time and acid concentration are shown in Table.4.2. Regression analysis was done to fit the response function as per the equation. From several possible models of Design expert7 software, a quadratic model was found to be adequate for the prediction of the given yield as shown by the following equation.

$$\text{Yield (Y)\%} = 37.71 - 1.9\text{A} - 2.58\text{B} - 0.7\text{C} - 2.46\text{AB} + 0.57\text{AC} + 0.22\text{BC}$$
$$-2.49A^2 - 2.26B^2 - 3.66C^2 \ldots\ldots\ldots\ldots\ldots\ldots\ldots\ldots \quad 4.1$$

Where all variables are indicated through the coded values. Table 4.2 shows the experimental and predicted results for the yield of CNCs obtained.

Table 4.2. BBD matrix of independent variables used in RSM with corresponding experimental and predicted values of response

Std	Run	Factors			Yield (%)	
		A: Temperature, ^{o}C	B: Time, min	C: Acid concentration, %	Actual	predicted
15	1	50.00	35.00	54.00	37.72	37.71
1	2	35.00	20.00	54.00	34.98	34.97
11	3	50.00	20.00	68.00	33.46	33.45
9	4	50.00	20.00	40.00	35.24	35.27
2	5	65.00	20.00	54.00	36.12	36.10
7	6	35.00	35.00	68.00	32.18	32.19
8	7	65.00	35.00	68.00	29.5	29.53
4	8	65.00	50.00	54.00	26.01	26.02
13	9	50.00	35.00	54.00	37.71	37.71
12	10	50.00	50.00	68.00	28.76	28.73
6	11	65.00	35.00	40.00	29.8	29.79
10	12	50.00	50.00	40.00	29.67	29.68
14	13	50.00	35.00	54.00	37.69	
3	14	35.00	50.00	54.00	34.72	
5	15	35.00	35.00	40.00	34.75	

The statistical significance of eqn (4.1) is tested by analysis of variance (ANOVA) results obtained from the quadratic BBD model as shown in Table 4.3. As suggested by the model F value and low probability value (p-value) which is less than 0.05, it is evidenced that the model is highly significant for this study. The P-value is a quantitative measurement for reporting the result of a tested hypothesis.

Table 4.3. Sequential Model Sum of Squares

Source	Sum of squares	df	Mean squares	F value	P value Prob>F	
Mean vs Total	16554.19	1	16554.19			
Linear vs Mean	85.99	3	28.66	2.98	0.078	
2FI vs Linear	25.73	3	8.577	0.86	0.501	
Quadratic vs 2FI	79.98	3	26.66	21444.34	< 0.0001	Suggested
Cubic vs Quadratic	0.0057	3	0.0019	8.21428571	0.1105	Aliased
Residual	0.00046	2	0.00023			
Total	16745.91	15	1116.39			

"Sequential Model Sum of Squares": Select the highest order polynomial where the additional terms are significant and the model is not aliased. In this case, the highest order polynomial is not needed since additional terms are not significant and the model is aliased.

Table 4.4. Results of lack of fit test

Source	Sum-of squares	df	Mean squares	F value	P value prob>F	
Linear	105.726	9	11.747	50345.82	< 0.0001	
2FI	79.993	6	13.332	57137.9	< 0.0001	
Quadratic	0.006	3	0.0019	8.214	0.1105	Suggested
Cubic	0	0				Aliased
Pure Error	0.000466	2	0.00023			

"Lack of Fit Tests": Want the selected model to have insignificant lack-of-fit.

Table 4.5. Results of Model Summary Statistics test

Source	Std. Dev.	R^2	Adjusted R^2	Predicted R^2	PRESS	
Linear	3.1002	0.4485	0.2981	0.1318	166.434	
2FI	3.1621	0.5827	0.2698	0.0935	173.79	
Quadratic	0.0352	0.998	0.979	0.895	0.093	Suggested
Cubic	0.0152	0.999	0.999		+	Aliased

+Case(s) with leverage of 1.0000: PRESS statistic not defined. "Model summary statistics": Focus on the model maximizing the "Adjusted R^2" and the "Predicted R^2". The predicted R-squared indicates the closeness of the factors for the model. As it approaches to unity means a good fit for the model selected which is quadratic model in this work. The standard deviation indicates the difference between each factors and grouped factor difference.

Table 4.6. Analysis of variance (partial sum of squares)

Source	Sum of Squares	df	Mean Squares	F value	P value Prob>F	
Model	191.71587	9	21.30	17132.78	< 0.0001	Significant
A-Temperature	28.88	1	28.88	23227.88	< 0.0001	
B-Time	53.2512	1	53.25	42829.38	< 0.0001	
C-Acid concentration	3.8642	1	3.86	3107.93	< 0.0001	
AB	24.255625	1	24.25	19508.54	< 0.0001	
AC	1.288225	1	1.28	1036.10	< 0.0001	
BC	0.189225	1	0.18	152.19	< 0.0001	
A^2	22.839077	1	22.83	18369.23	< 0.0001	
B^2	18.893616	1	18.89	15195.93	< 0.0001	
C^2	49.517000	1	49.51	39826.0	< 0.0001	
Residual	0.0062166	5	0.001			
Lack of Fit	0.00575	3	0.0019	8.21	0.1105	not significant
Pure Error	0.0004666	2	0.087		< 0.0001	
Cor Total	134.41	14			< 0.0001	

The significant of the coefficient term is determined by the value of F and p, and the larger the value of F and the smaller the value of p, the more significant is the model. The Model F-value of 17132.78 implies the model is significant. There is only a 0.010% chance that a "Model F-Value" this large could occur due to noise. Values of "Prob > F" less than 0.0500 indicate model terms are significant. In this case A, B, C, AB, AC, BC, A^2, B^2, C^2 are significant model terms. Values greater than 0.1000 indicate the model terms are not significant. The "Lack of Fit F-value" of 8.21 implies there is a 11.05% chance that a "Lack of Fit F-value" this large could occur due to noise. Lack of fit is bad -- we want the model to fit. This relatively low probability (<10%) is troubling. The adequacy of the model was also evaluated by the residuals which is difference between the observed and the predicted response values. Residuals are thought of as elements of variation unexplained by the fitted model and then it is expected that they occur according to a normal distribution.

Table 4.7. Results of R-Squared Test

Std. Dev.	0.035261	R^2	0.998
Mean	33.22067	Adj R^2	0.979
C.V. %	0.106142	Pred R^2	0.895
PRESS	0.09305	Adeq Precision	406.09

Multiple regression coefficients R^2 is calculated from the second-degree polynomial equation given in eqn (4.1) is 0.998. This indicates that the predicted values are closer to experimental data and the quadratic polynomial was capable of representing the system for the given experimental domain. The closer the R^2 value to unity, the stronger the model and the better it predicts the response. Adeq Precision measures the signal to noise ratio. A ratio greater than 4 is desirable. For this work, ratio of 406.09 indicates an adequate signal. Therefore, this model can be used to navigate the design space. A lower value of coefficient of variation, CV = 0.106% indicates the precision with which the experiments were conducted. Similarly, the smaller predicted residual sum of squares (PRESS) statistic shows the better data points fit the model. Normal probability plots are also a suitable graphical method for judging the normality of the residuals. A normal plot of residuals

between the normal probability (%) and the internally studentized residuals was obtained to determine how well the model satisfies the assumptions of ANOVA. The internally studentized residuals can also be used to measure the standard deviations separating the experimental and predicted values. Figure 4.8 shows the relationship between the normal probability (%) and the internally studentized residuals. The straight line means that no response transformation was required and that there was no apparent problem with normality.

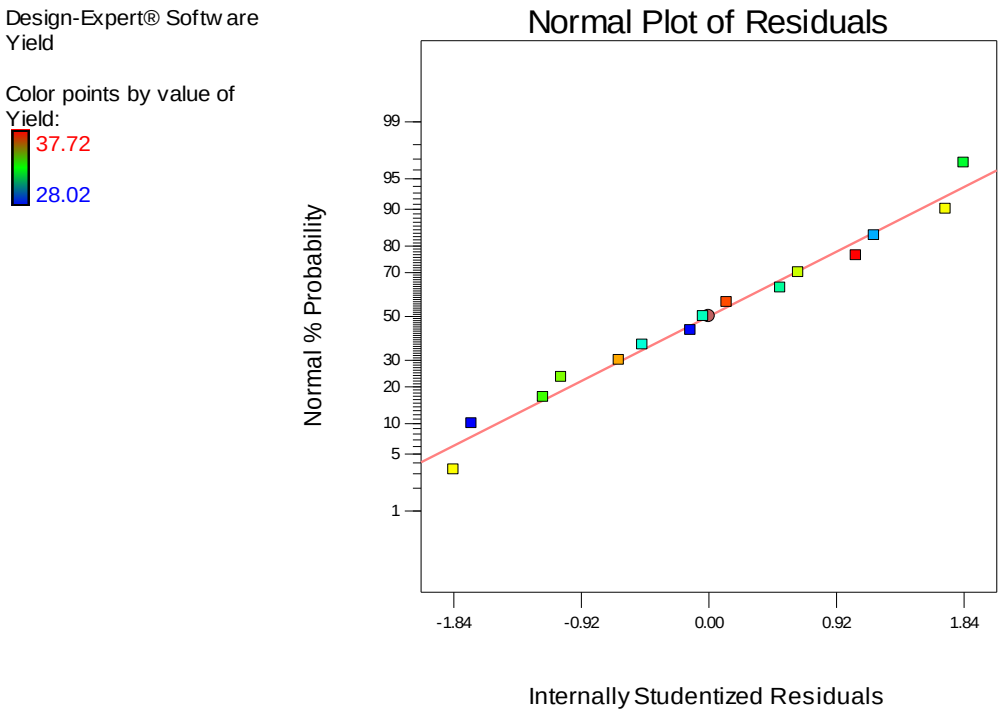

Figure 4.8. Normal plot of residuals experimental values

The observed residuals were also plotted against the expected values, given by a normal distribution as shown in Figure 4.9. The approximate straight lines obtained indicate that residuals are normally distributed and the residuals appeared to be randomly scattered.

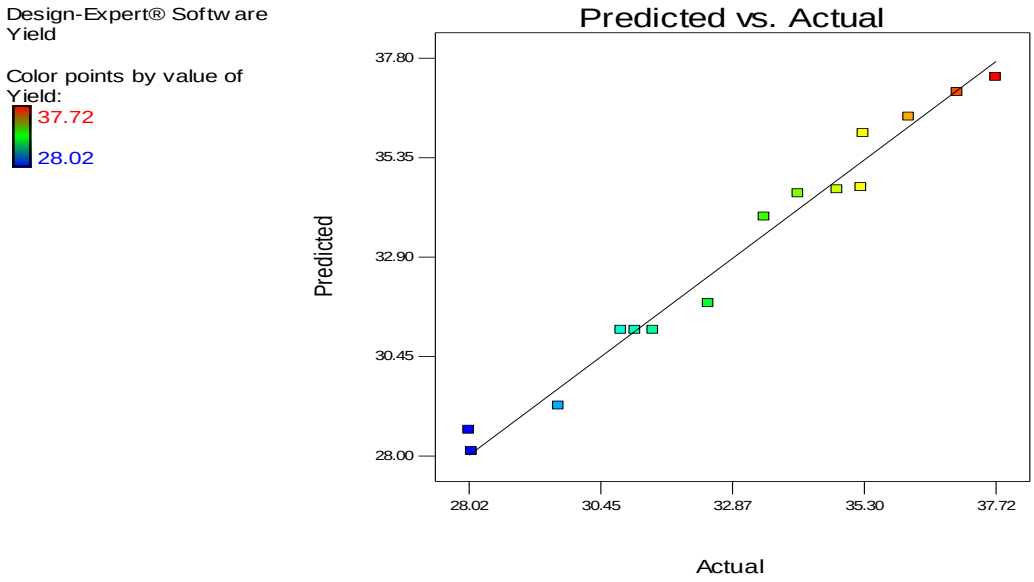

Figure 4.9. Predicted vs. actual plot of response values

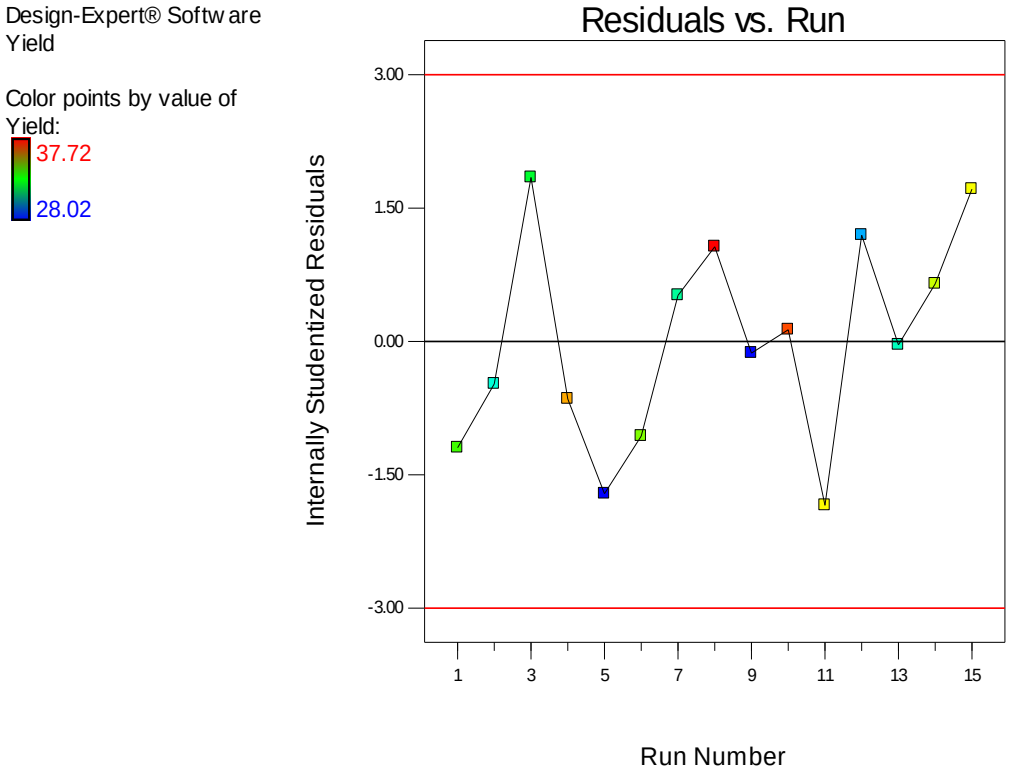

Figure 4.10. Plot of internally studentized residuals versus run number

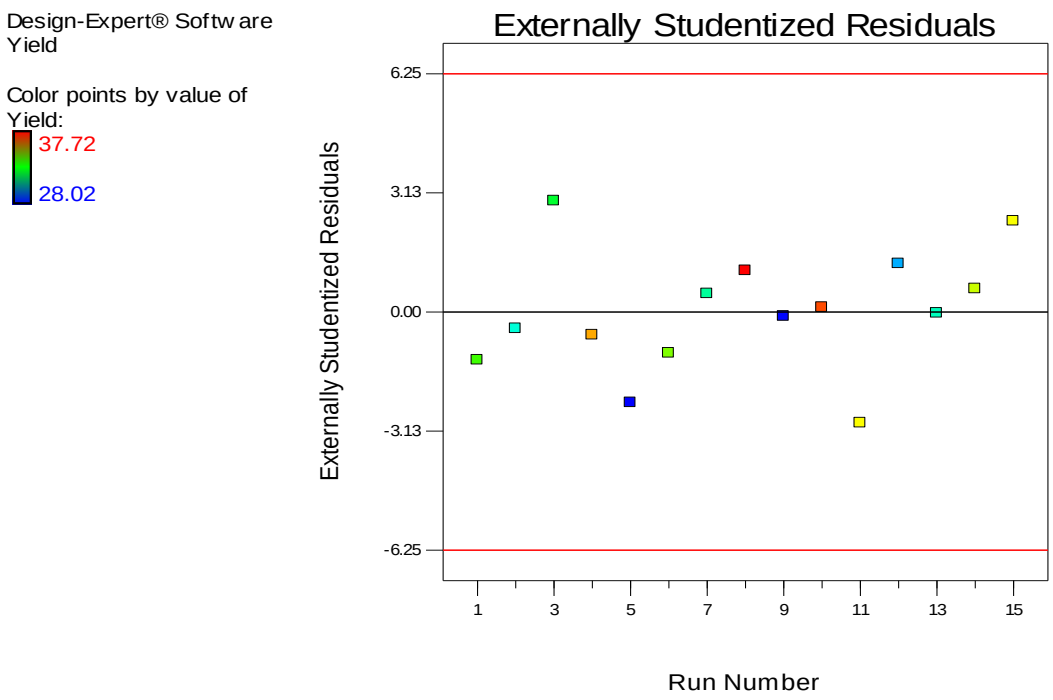

Figure 4.11. Plot of externally studentized residuals versus run numbers

4.5 Effects of parameters on the yield of crystalline nanocellulose

4.5.1 Effects of temperature on yield of CNCs

Figure 4.12 shows the individual effects of hydrolysis temperature on the response of the study by keeping other two parameters at their values that gives the maximum yield. It was observed that at the lower level of temperature, the yield is lower and increased with increasing the temperature since the increment of the temperature enhance the hydrolysis reaction at the starting of the reaction. After it reaches the optimum value at around 50 ^{o}C, increasing the temperature lower the values of the yield due to the over degradation of cellulose as temperature further increased. Higher level of temperature, cellulose molecules undergo over degradation and as a result undesired product can formed. The negative value of regression coefficient of temperature indicates how the temperature negatively affect the response after optimum point and agrees with the relation shown by Figure 4.12. Therefore, operating at around 50 ^{o}C of temperature with suitable values of other parameter can give the optimum yield.

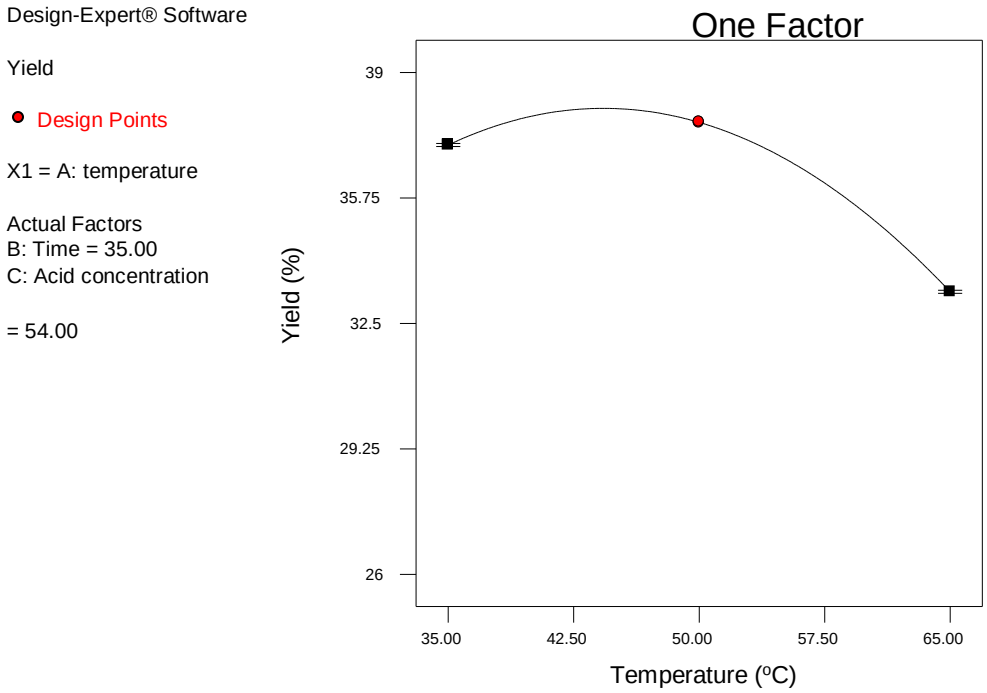

Figure 4.12. Effect of temperature on response at constant time and acid concentration

4.5.2 Effect of hydrolysis time on the yield of CNC

Similarly, the yield of CNCs was negatively affected by hydrolysis time as shown from Figure 4.13 and regression coefficient of time given in eqn (4.1).

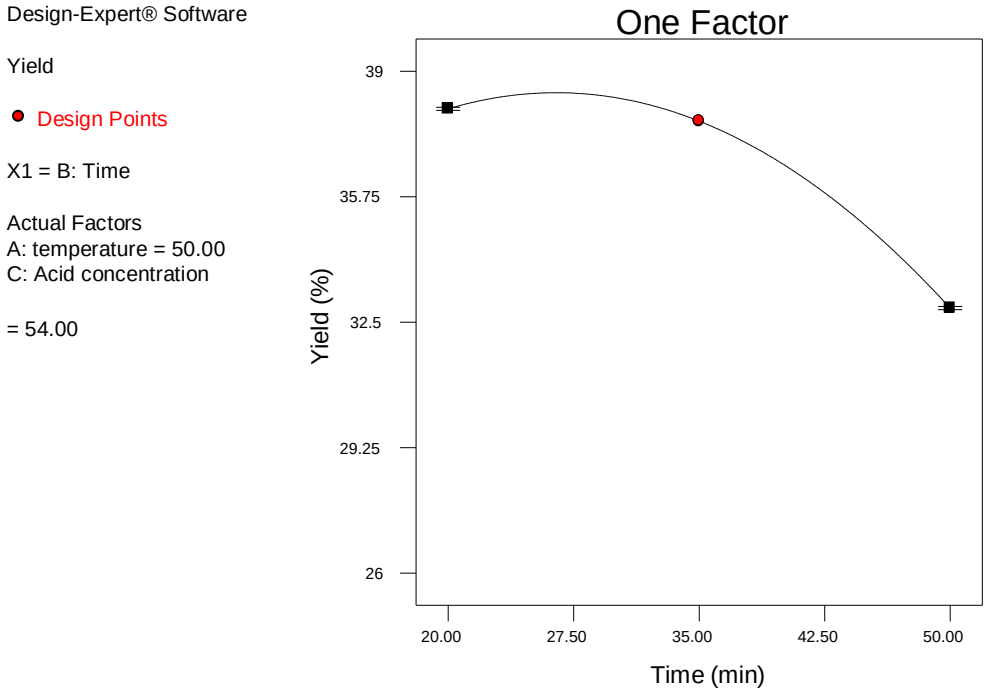

Figure 4.13. Effect of hydrolysis time on the yield of CNCs

It was observed that the maximum value of yield was obtained at the lower level of time and decreased with increased values of time, while other parameters were kept at their fixed values where maximum yield was obtained. As the operating time increased, the cellulose and nanocellulose produced can degrade further and results in the decrease of the CNCs yield.

4.5.3 Effect of acid concentration on the yield of CNCs

The yield of CNCs is increased at the starting of hydrolysis with increasing acid concentration. This is due to the high penetration of acid to the amorphous part of cellulose which enhance the conversion of cellulose to CNCs. The yield reaches its optimum at acid concentration of 54 % and then decreased with further increasing of acid concentration due to the over degradation of cellulose to undesired products.

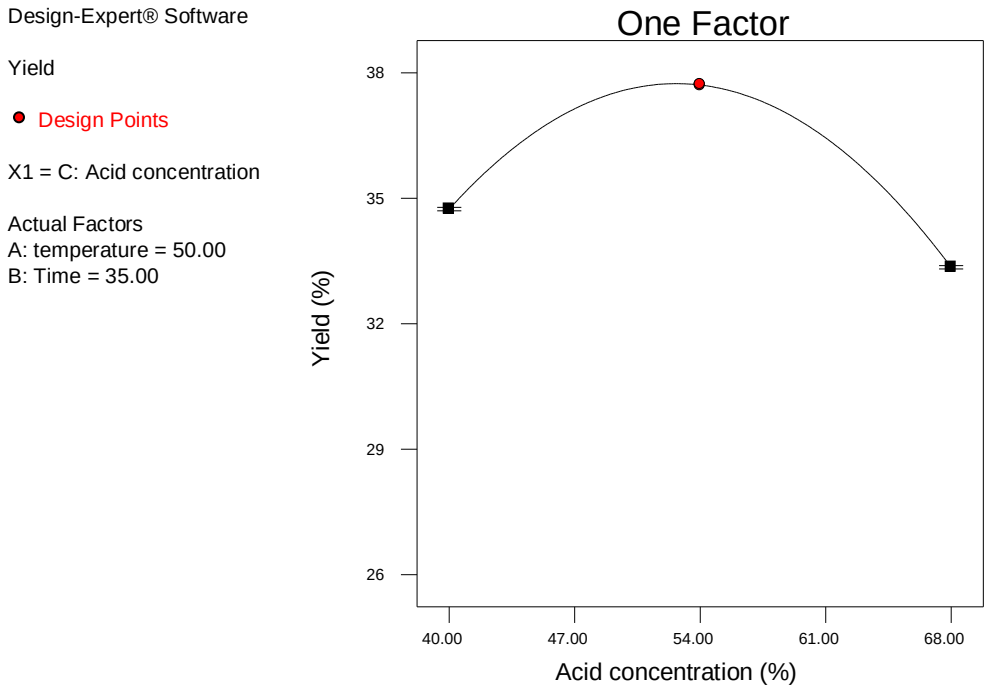

Figure 4.14. Effect of acid concentration on the yield of CNCs

4.5.4 Interaction effect of temperature and time on the yield of CNC

The interaction of temperature and time has significant effect on the yield of CNCs as shown in Figure 4.15. It was observed that the yield was increased with increasing temperature and decreasing time at the starting of hydrolysis reaction. At lower temperature level, the variation of hydrolysis time had less effect on the variation of the yield. However, at the higher level of temperature the yield was highly affected by the variation of the time

in such a way that the yield was highly decreased with increasing the time. This is happened due to the over degradation of cellulose to undesired products at higher level of both temperature and time

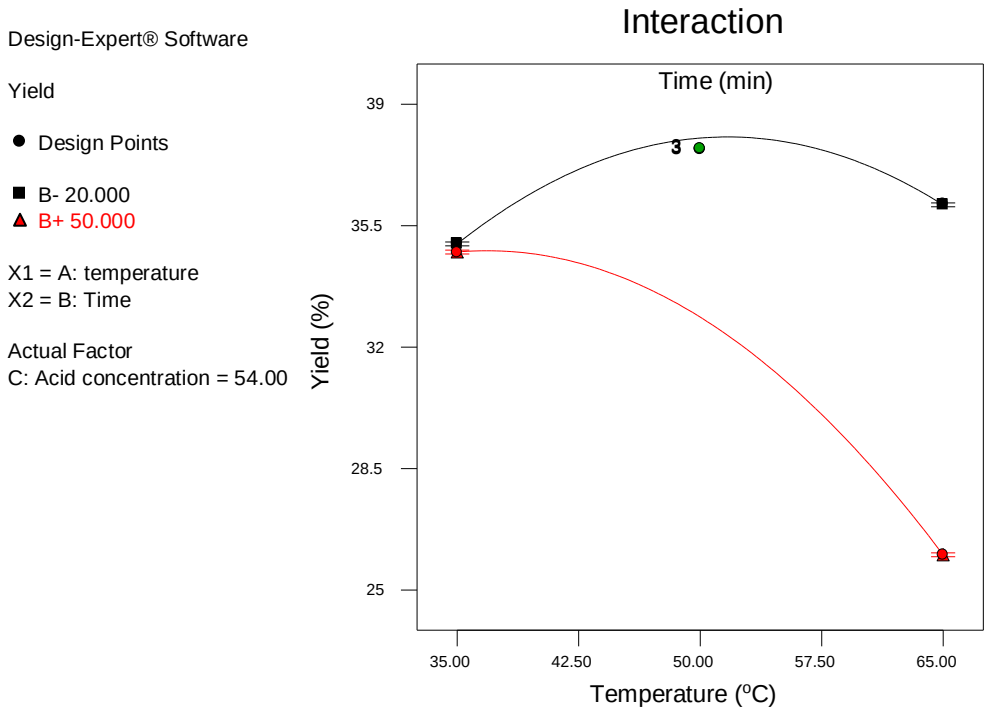

Figure 4.15. Interaction effects of temperature and time on the yield of CNCs

4.5.5 Interaction effects of temperature and acid concentration on the yield of CNCs

The interaction of temperature and acid concentration negatively affect the yield of CNCs after its optimum point as shown in Figure 4.16. The relationship of their interaction and yield was also shown from the regression coefficient of their interaction in eqn (4.1). The curves of the plot shown in Figure 4.16 are not parallel. This shows that the interaction of temperature and acid concentration has higher effect on the yield than other possible interaction. It was observed that at lower level of temperature, lower value of acid concentration gives high yield and decreased with increasing temperature. However, at higher level of temperature the variation of acid concentration has no significant effect. It was also observed that the effect of acid concentration variation on the yield at the lower level of temperature was high than that observed at the higher level of temperature.

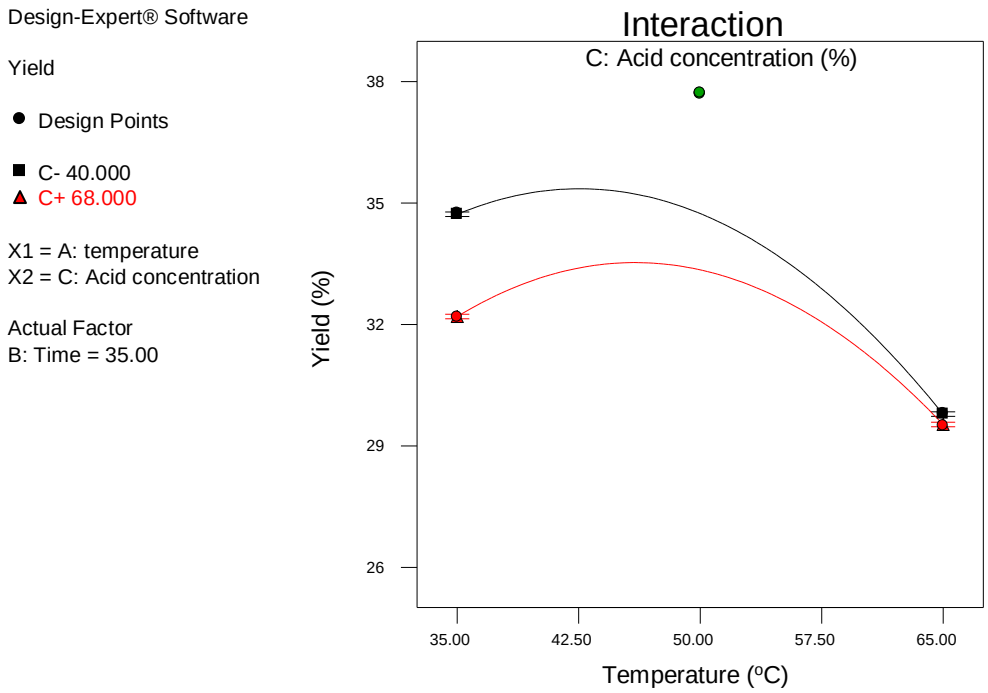

Figure 4.16. Interaction effect of temperature and acid concentration on the yield of CNCs

4.5.6 Interaction effect of time and acid concentration on yield

The curves of time and acid concentration shown in the plot of Figure 4.17 are nearly parallel to each other showing their interaction effect on the yield at a constant reaction temperature.

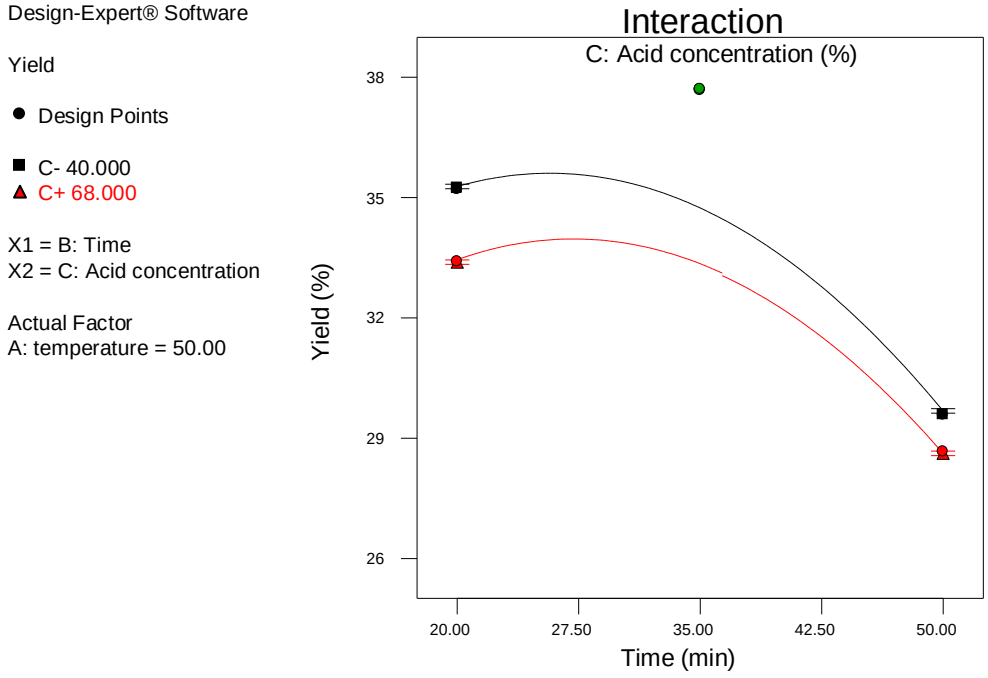

Figure 4.17. Interaction effect of time and acid concentration on the yield of CNCs

From Figure 4.17, it is shown that the interaction effects of time and acid concentration on the yield of CNCs is not highly significant as compared to other interaction. It is observed that the lower acid concentration gives higher yield at the both lower level and higher level of time and decreased with increasing hydrolyzing time. This is due to the over degradation of cellulose to undesired products as both time and acid concentration increased.

4.5.7 Response surface and contour plot for yield with parameter interaction

The individual and cumulative effects as well as the mutual interactions between the parameters on the dependent variables were described using response surface and contour plots. In this study, the response surface and contour plots were described by the regression model for BBD which was developed using Design-expert 7.0.0 software. Figure 4.18 shows the effect of temperature and time on the yield of CNCs at fixed value of acid concentration. It was observed that the yield of CNCs increased with increasing hydrolysis time to 35 min and the temperature to 50 ^{o}C at which the optimum yield was obtained. At the higher-level temperature and time, the yield was lower due to the over degradation of cellulose to undesired products.

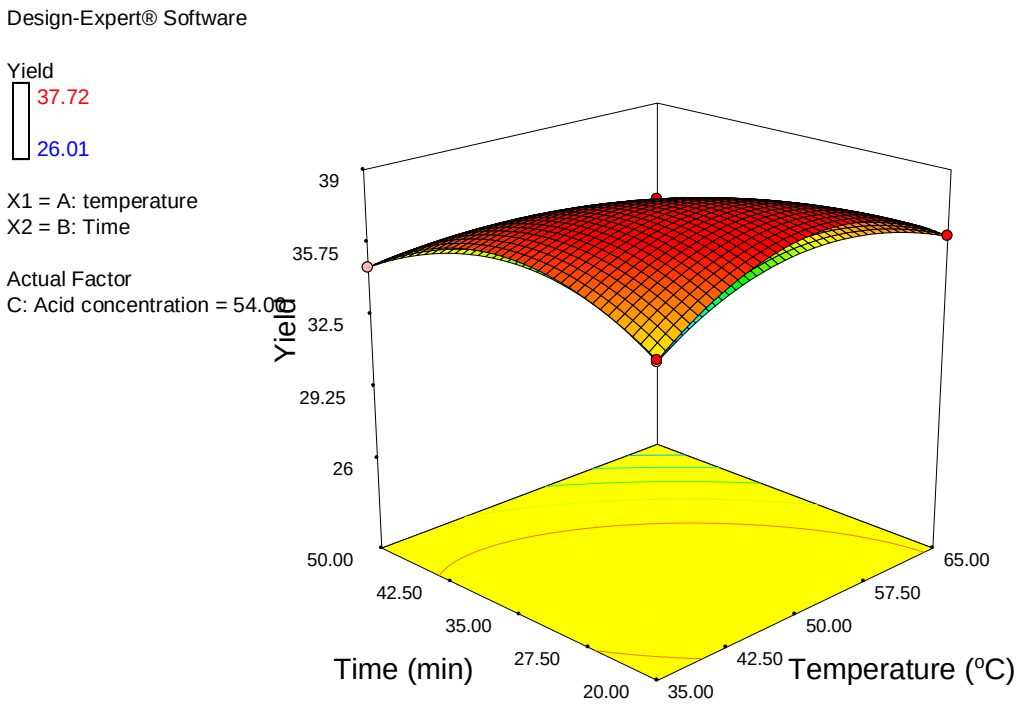

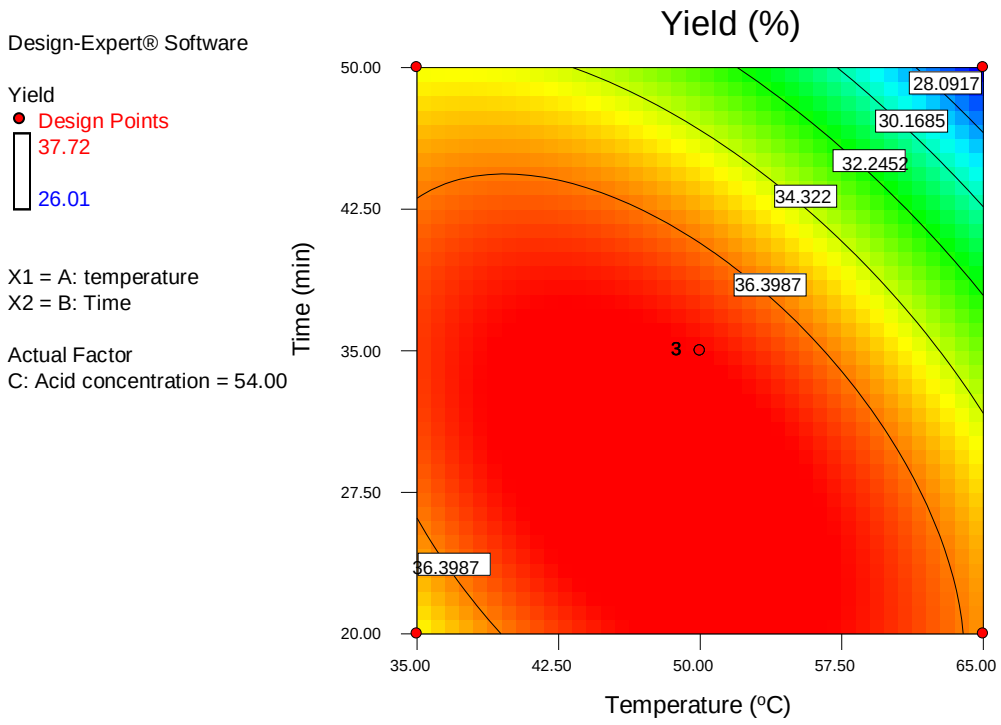

Figure 4.18. Response surface and contour plot showing interaction effect of temperature and time on the yield of CNCs

Figure 4.19 shows the effect of temperature and acid concentration at a fixed value of acid concentration. From Figure 4.19, it was observed that the yield of CNC was increased with increasing acid concentration to 54 % and temperature to 50 ^{o}C at which the optimum yield was obtained. However, further increasing of both acid concentration and temperature results in the decrement of CNCs yield due to the over degradation of cellulose to undesired products.

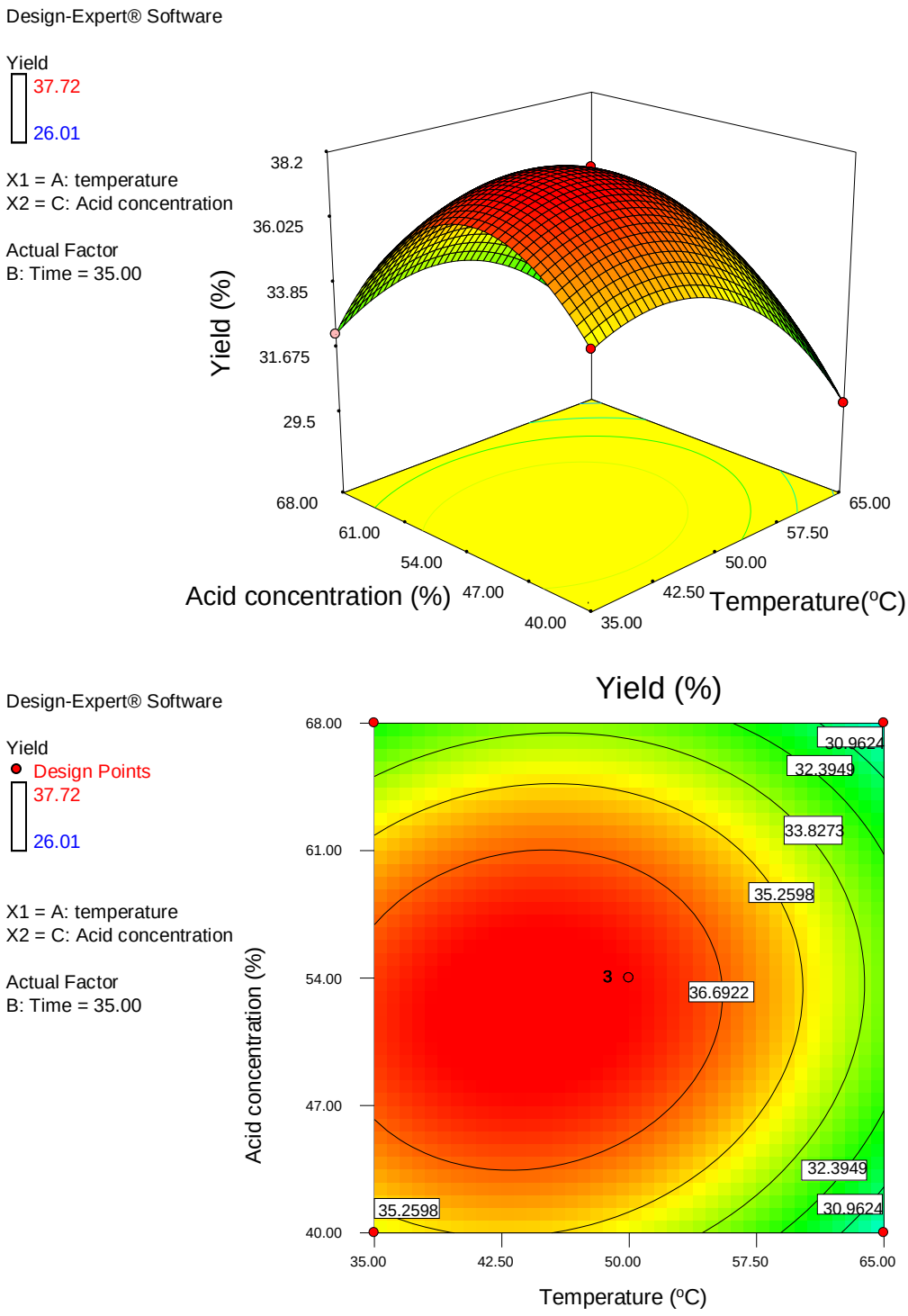

Figure 4.19. Response surface and contour plot showing interaction of temperature and acid concentration

Figure 4.20 shows the response surface plot with the interaction effect of time and acid concentration at affixed value of temperature.

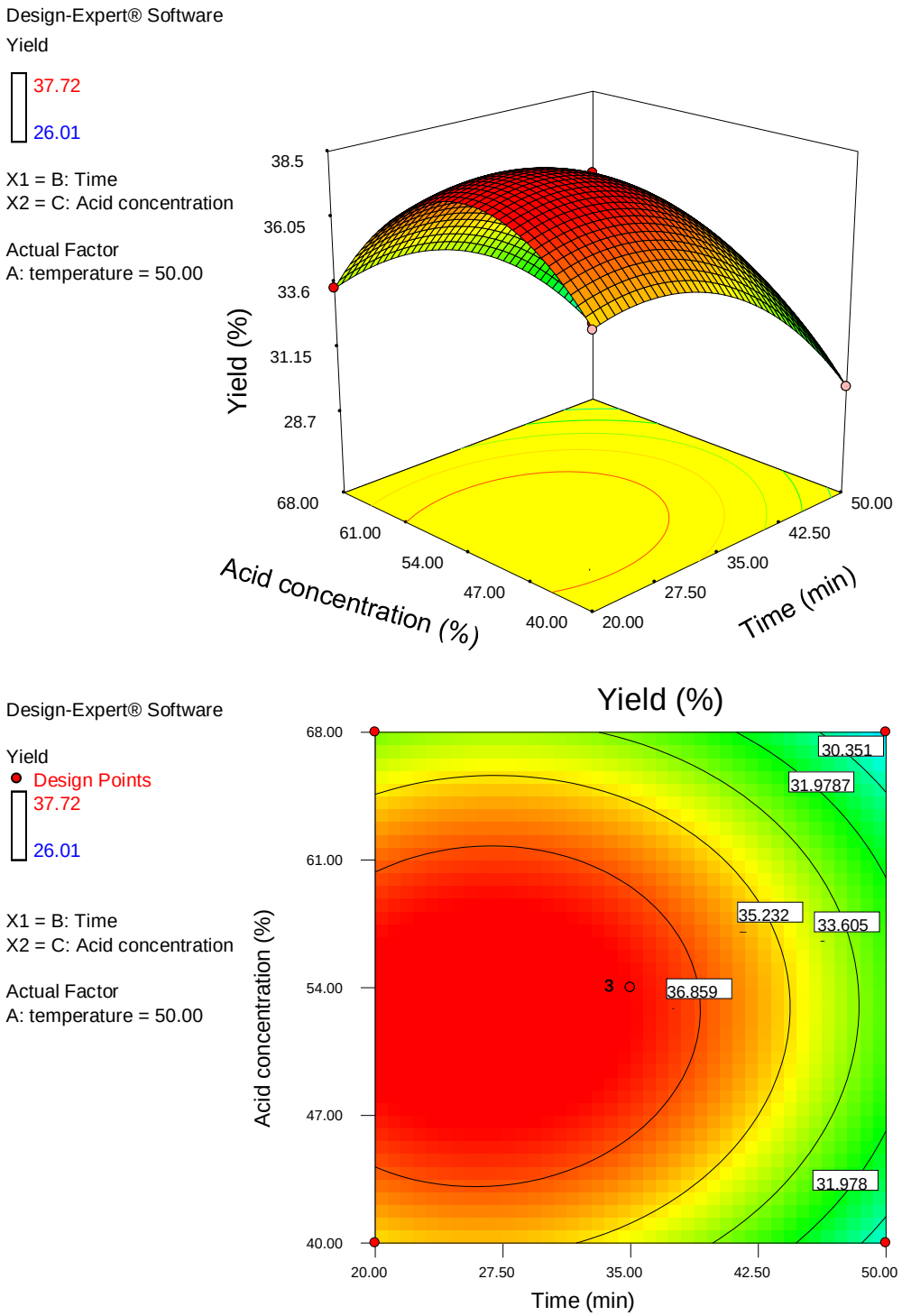

Figure 4.20. Response surface and contour plot for time and acid concentration interaction

It was observed that the yield was increased with increasing acid concentration and time at their meddle values at which the optimum yield was obtained and decreased with further increasing of hydrolysis time and acid concentration. At higher level of acid concentration and time the cellulose molecules can undergo over degradation to undesired products.

4.6 Optimization of the model and process parameters

Optimization of the response surface is used to find the desirable location such as maximum, minimum of an area with stable response in a given design space and range of process parameters. In this study, design-expert 7.0.0 software was used for the purpose of response analysis and optimization. The criterion of optimization for the selection of the optimal operating conditions using the quadratic BBD based model was to get the maximum CNCs yield with the process factors constrained to the applied experimental region. Numerical optimization, graphical optimization and point prediction are ways of expressing optimum process condition and its result. However, all of these optimization methods give similar optimized values for process parameters and the results. Table 4.8 shows possible solutions of numerical optimization with different values of desirability. As shown from the Table, the values of desirability are varied from zero to one and shows the location of maximized responses. The unit value of desirability implies that some of the solutions are located beyond the specified upper limit. According to the experimental work done, the maximum yield of 37.72 % was obtained at the interaction parameter of 50 ^{o}C, 35 min and 54 % of acid concentration. Under this condition of parameter interaction, the predicted yield of CNCs obtained was 37.71%. This shows that the predicted values of the CNCs yield agreed with that obtained from experimental work. From response optimization technique used in this study, the yield of CNCs was optimized to 38.4057 % at a desirable parameter interaction of 45.94 ^{o}C, 26.94 min and 50.2 % acid concentration as shown in Table 4.8.

Table 4.8. Solutions of numerical optimization with optimum process conditions and response

Number	Temperature	Time	Acid concentration	Yield	desirability	
1	45.94	26.94	50.2	38.4057	1	Selected
2	52.17	24.46	53.78	38.337	1	
3	41.56	32.78	49.96	38.112	1	
4	41.38	34.31	49.03	37.931	1	
5	44.26	34.36	50.45	38.134	1	
6	42.07	32.3	54.97	38.084	1	
7	40.17	33.86	54.87	37.862	1	
8	45.33	26.67	52.76	38.421	1	
9	57	21.67	53.38	37.826	1	
10	40.48	28.33	55.52	37.748	1	
11	57	21.67	51.51	37.801	1	
12	43.25	34.95	55.24	37.949	1	
13	46.67	31.67	52.13	38.397	1	

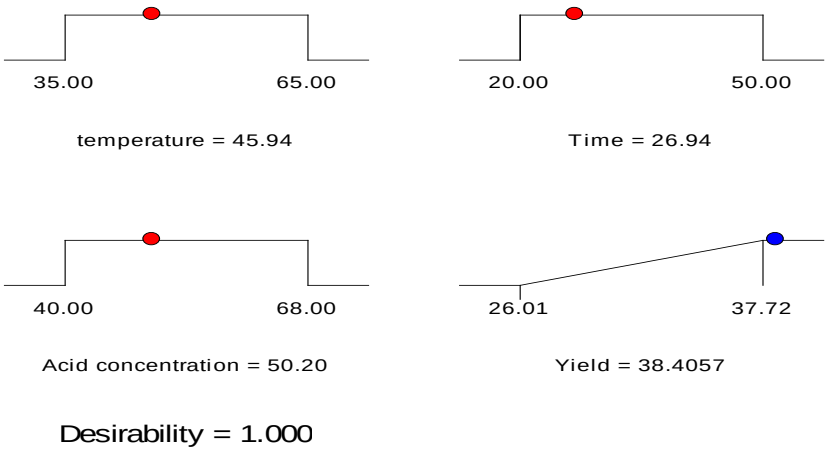

Figure 4.21. Ramps numerical optimization of parameters and response

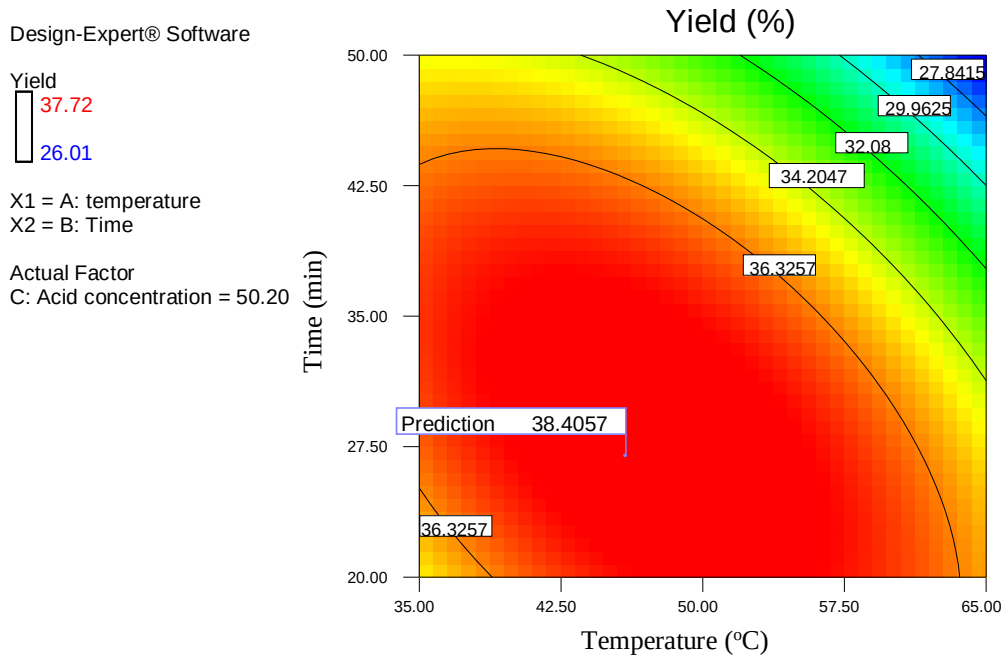

Figure 4.22. contour of numerical optimization process parameters and the yield of CNCs

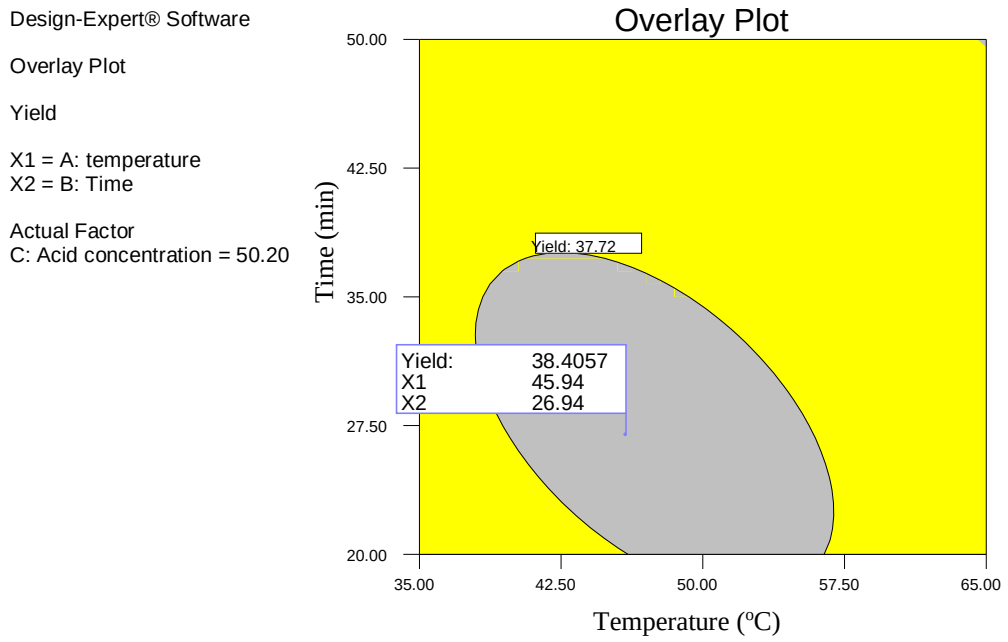

Figure 4.23. Overlay plot of graphical optimization of process parameters and response

Table 4.9. Point prediction optimization of process parameter and response

Factor	Name	Level	Low Level	High Level	Std. Dev.	Coding	
A	Temperature	45.9382716	35	65	0	Actual	
B	Time	26.9382716	20	50	0	Actual	
C	Acid concentration	50.1975309	40	68	0	Actual	
Response Yield	Prediction 38.4057	SE Mean 0.0187	95% CI low 38.357	95% CI high 38.454	SE Pred 0.0399	95% PI low 38.303	95% PI high 38.508

After optimization, triplicate experiments were performed using these optimized process conditions. At this condition, the mean percentage of yield obtained was 38.37% and which was then related to the data obtained from optimization analysis using desirability function.

5. Conclusion and Recommendation

5.1 Conclusion

Cellulose nanocrystalline (CNCs) was isolated from water hyacinth using acid hydrolysis methods. Soxhlet extraction, alkaline treatment and bleaching steps are the most necessary pretreatment steps to isolate purified cellulose for acid hydrolysis. The result of sample characterization showed that the obtained CNCs have whisker-shaped structure with an average diameter of 102.6 nm showing high thermal stability. It was also observed that non-cellulosic components were removed with pretreatment steps as proved from ATR-FTIR analysis. The yield of CNCs was affected by selected operating parameters such as hydrolysis temperature, time and acid concentration. The yield is negatively affected by temperature and time while acid concentration has direct effect in the case of one parameter effect. From the interaction effect, the yield was highly affected by the interaction of temperature and acid concentration. Maximum yield of 37.72% was obtained at the parameter interaction of 50 ^{o}C, 35 min and 54 % of acid concentration. The obtained result was optimized to 38.4057% which is obtained at 45.94 ^{o}C, 26.94 min and 50.2% acid concentration using RSM. Generally, the study has demonstrated that water hyacinth can serves as a best biomass feedstock for producing CNCs with a powerful application and alternative way for reducing the negative effects of water hyacinth on environment.

5.2 Recommendation

From different parts of water hyacinth such as stem, root and leaves, only stem was used as a source of cellulose. But, leave and root of water hyacinth have also cellulose and other components which can be used as feedstocks for different value-added materials. So, it is recommended that other parts of this plant should also tested for better purpose rather than dispose it on landfill. For producing nanocellulose from lignocellulosic biomass, pretreatments are the most important and recommended steps to get purified cellulose. During extraction and pretreatment steps, extractive components, lignin and hemicellulose were removed from lignocellulosic biomass which were then washed out. It is better and recommended to recover and change these components to value added material as much as possible. There are different factors that can affect the yield of nanocellulose during acid hydrolysis. In this study, only the effects of temperature, hydrolysis time and acid concentration on yield were tested. Therefore, other parameters such as solid cellulose to acid ratio that can affect the yield and properties of nanocellulose should also be tested and optimized.

References

Abdul Khalil, H. P. S., Davoudpour, Y., Saurabh, C. K., Hossain, M. S., Adnan, A. S., Dungani, R., … Haafiz, M. K. M. (2016, October). A review on nanocellulosic fibres as new material for sustainable packaging: Process and applications. *Renewable and Sustainable Energy Reviews*, Vol. 64, pp. 823–836.

Abdul Latif, M. H., & Mahmood, Y. F. (2018). Isolation and Characterization of Microcrystalline Cellulose and Preparation of Nano-Crystalline Cellulose from Tropical Water Hyacinth. *Ibn AL- Haitham Journal For Pure and Applied Science*, *31*(1), 180.

Abitbol, T., Rivkin, A., Cao, Y., Nevo, Y., Abraham, E., Ben-Shalom, T., … Shoseyov, O. (2016). Nanocellulose, a tiny fiber with huge applications. *Current Opinion in Biotechnology*, *39*(I), 76–88.

Akendo, I. C. O., Gumbe, L. O., & Gitau, A. N. (2008). Dewatering and Drying Characteristics of Water Hyacinth (Eichhornia crassipes) Petiole . Part I . Dewatering Characteristics. *Agricultural Engineering International*, *X*, 1–14.

Asrofi, M., Abral, H., Kasim, A., Pratoto, A., Mahardika, M., & Hafizulhaq, F. (2018). Mechanical Properties of a Water Hyacinth Nanofiber Cellulose Reinforced Thermoplastic Starch Bionanocomposite: Effect of Ultrasonic Vibration during Processing. *Fibers*, *6*(2), 40.

Asrofi, M., Abral, H., Kasim, A., Pratoto, A., Mahardika, M., Park, J.-W., & Kim, H.-J. (2018). Isolation of Nanocellulose from Water Hyacinth Fiber (WHF) Produced via Digester-Sonication and Its Characterization. *Fibers and Polymers*, *19*(8), 1618–1625.

B, S., & A, D. R. (2016). A Study on Chemical Analysis of Water Hyacinth (Eichornia crassipes), Water Lettuce (Pistia stratiotes). *International Journal of Innovative Research in Science, Engineering and Technology*, *5*(10), 17566–17570.

Bhat, A. H., Dasan, Y. K., Khan, I., Soleimani, H., & Usmani, A. (2017). Application of nanocrystalline cellulose. In *Cellulose-Reinforced Nanofibre Composites* (pp. 215–240).

C.S., J. C., George, N., & Narayanankutty, S. K. (2016). Isolation and characterization of cellulose nanofibrils from arecanut husk fibre. *Carbohydrate Polymers*, *142*, 158–166.

Chen, Y. W., Lee, H. V., Juan, J. C., & Phang, S. M. (2016). Production of new cellulose nanomaterial from red algae marine biomass Gelidium elegans. *Carbohydrate Polymers*, *151*, 1210–1219.

Chirayil, C. J., Mathew, L., & Thomas, S. (2014). Review of recent research in nano cellulose preparation from different lignocellulosic fibers. *Reviews on Advanced Materials Science*, Vol. 37, pp. 20–28.

El Achaby, M., Kassab, Z., Aboulkas, A., Gaillard, C., & Barakat, A. (2018). Reuse of red algae waste for the production of cellulose nanocrystals and its application in polymer nanocomposites. *International Journal of Biological Macromolecules*, *106*, 681–691.

Endes, C., Camarero-Espinosa, S., Mueller, S., Foster, E. J., Petri-Fink, A., Rothen-Rutishauser, B., … Clift, M. J. D. (2016). A critical review of the current knowledge regarding the biological impact of nanocellulose. *Journal of Nanobiotechnology*, *14*(1), 78.

Fortunati, E., Luzi, F., Puglia, D., & Torre, L. (2016). Extraction of Lignocellulosic Materials From Waste Products. In *Multifunctional Polymeric Nanocomposites Based on Cellulosic Reinforcements* (pp. 1–38).

George, J., & S N, S. (2015). Cellulose nanocrystals: synthesis, functional properties, and applications. *Nanotechnology, Science and Applications*, *8*, 45.

Ghazy, M. B., Esmail, F. A., El-Zawawy, W. K., Al-Maadeed, M. A., & Owda, M. E. (2016). Extraction and characterization of Nanocellulose obtained from sugarcane bagasse as agro-waste. *Journal Of Advances In Chemistry*, *12*(3), 4256–4264.

Herrera Rodriguez, M. (2015). *Preparation and Characterization of Nanocellulose Films and Coatings from Industrial Bio-Residues*.

Hutomo, G. S., Rahim, A., & Kadir, S. (2015). The Effect of Sulfuric and Hydrochloric Acid on Cellulose Degradation from Pod Husk Cacao. *International Journal on*

Current Microbiology and Applied Sciences, *4*(10), 89–95.

Jiang, F., & Hsieh, Y.-L. (2015). Cellulose nanocrystal isolation from tomato peels and assembled nanofibers. *Carbohydrate Polymers*, *122*, 60–68.

Jiang, Y., Zhou, J., Zhang, Q., Zhao, G., Heng, L., Chen, D., & Liu, D. (2017). Preparation of cellulose nanocrystals from Humulus japonicus stem and the influence of high temperature pretreatment. *Carbohydrate Polymers*, *164*, 284–293.

Kallel, F., Bettaieb, F., Khiari, R., García, A., Bras, J., & Chaabouni, S. E. (2016). Isolation and structural characterization of cellulose nanocrystals extracted from garlic straw residues. *Industrial Crops and Products*, *87*, 287–296.

Kargarzadeh, H., Mariano, M., Huang, J., Lin, N., Ahmad, I., Dufresne, A., & Thomas, S. (2017). Recent developments on nanocellulose reinforced polymer nanocomposites: A review. *Polymer*, *132*, 368–393.

Kim, D.-Y., Lee, B.-M., Koo, D. H., Kang, P.-H., & Jeun, J.-P. (2016). Preparation of nanocellulose from a kenaf core using E-beam irradiation and acid hydrolysis. *Cellulose*, *23*(5), 3039–3049.

Kim, D. Y., Lee, B. M., Koo, D. H., Kang, P. H., & Jeun, J. P. (2016). Preparation of nanocellulose from a kenaf core using E-beam irradiation and acid hydrolysis. *Cellulose*, *23*(5), 3039–3049.

Lee, H. V., Hamid, S. B. A., & Zain, S. K. (2014). Conversion of Lignocellulosic Biomass to Nanocellulose: Structure and Chemical Process. *The Scientific World Journal*, *2014*, 1–20.

Liu, C., Li, B., Du, H., Lv, D., Zhang, Y., Yu, G., … Peng, H. (2016). Properties of nanocellulose isolated from corncob residue using sulfuric acid, formic acid, oxidative and mechanical methods. *Carbohydrate Polymers*, *151*, 716–724.

Lu, P., & Hsieh, Y.-L. (2012). Preparation and characterization of cellulose nanocrystals from rice straw. *Carbohydrate Polymers*, *87*(1), 564–573.

Malucelli, L. C., Lacerda, L. G., Dziedzic, M., & da Silva Carvalho Filho, M. A. (2017). Preparation, properties and future perspectives of nanocrystals from agro-industrial

residues: a review of recent research. *Reviews in Environmental Science and Bio/Technology*, *16*(1), 131–145.

Marimuthu, T. S., & Atmakuru, R. (2015). Isolation and Characterization of Cellulose Nanofibers from the Aquatic Weed Water Hyacinth: Eichhornia crassipes. In *Handbook of Polymer Nanocomposites. Processing, Performance and Application* (Vol. 87, pp. 37–46).

Mariño, M., Lopes da Silva, L., Durán, N., & Tasic, L. (2015). Enhanced Materials from Nature: Nanocellulose from Citrus Waste. *Molecules*, *20*(4), 5908–5923.

Mashego, D. V. (2016). *Preparation , Isolation and Characterization of Nanocellulose From Sugarcane Bagasse*. (August).

Mishra, R. K., Sabu, A., & Tiwari, S. K. (2018). Materials chemistry and the futurist eco-friendly applications of nanocellulose: Status and prospect. *Journal of Saudi Chemical Society*, *22*(8), 949–978.

Missoum, K., Belgacem, M., & Bras, J. (2013). Nanofibrillated Cellulose Surface Modification: A Review. *Materials*, *6*(5), 1745–1766.

Mondal, S. (2017). Preparation, properties and applications of nanocellulosic materials. *Carbohydrate Polymers*, *163*, 301–316.

Morais, J. P. S., Rosa, M. D. F., de Souza Filho, M. de sá M., Nascimento, L. D., do Nascimento, D. M., & Cassales, A. R. (2013). Extraction and characterization of nanocellulose structures from raw cotton linter. *Carbohydrate Polymers*, *91*(1), 229–235.

Mukhopadhyay, S., & Chatterjee, N. C. (2010). Bioconversion of water hyacinth hydrolysate into ethanol. *BioResources*, *5*(2), 1301–1310.

Nascimento, P., Marim, R., Carvalho, G., & Mali, S. (2016). Nanocellulose Produced from Rice Hulls and its Effect on the Properties of Biodegradable Starch Films. *Materials Research*, *19*(1), 167–174.

Navarro, L., & Phiri, G. (2000). *Water hyacinth in Africa and the Middle East: a survey of problems and solutions*. Retrieved from

Nguyen Thi, B. T., Ong, L. K., Nguyen Thi, D. T., & Ju, Y.-H. (2017). Effect of subcritical water pretreatment on cellulose recovery of water hyacinth (Eichhornia crassipe). *Journal of the Taiwan Institute of Chemical Engineers*, *71*, 55–61.

Oksman, K., Aitomäki, Y., Mathew, A. P., Siqueira, G., Zhou, Q., Butylina, S., … Hooshmand, S. (2016). Review of the recent developments in cellulose nanocomposite processing. *Composites Part A: Applied Science and Manufacturing*, *83*, 2–18.

Oliveira, F. B. de, Bras, J., Pimenta, M. T. B., Curvelo, A. A. da S., & Belgacem, M. N. (2016). Production of cellulose nanocrystals from sugarcane bagasse fibers and pith. *Industrial Crops and Products*, *93*, 48–57.

Oun, A. A., & Rhim, J. W. (2016). Isolation of cellulose nanocrystals from grain straws and their use for the preparation of carboxymethyl cellulose-based nanocomposite films. *Carbohydrate Polymers*, *150*, 187–200.

Phanthong, P., Reubroycharoen, P., Hao, X., Xu, G., Abudula, A., & Guan, G. (2018). Nanocellulose: Extraction and application. *Carbon Resources Conversion*, *1*(1), 32–43.

Pitaloka, A. B., Saputra, A. H., & Nasikin, M. (2013). Water hyacinth for superabsorbent polymer material. *World Applied Sciences Journal*, *22*(5), 747–754.

R., T. (2000). Water hyacinth paper. Contribution to a sustainable future Paper and Water. *Rijswijk, Gentenaar & Torley Publishers*, 1–12.

Ranganath, M. S. (2015). *Surface Roughness Prediction Model for CNC Turning of EN-8 Steel Using Response Surface Methodology*. *5*(6), 135–143.

Rezania, S., Fadhil, M., Din, M., Mohamad, S. E., Sohaili, J., Taib, S. M., … Ahsan, A. (2017). Review on Pretreatment Methods and Ethanol Production from Cellulosic Water Hyacinth. *BioResources*, *12*(1), 2108–2124.

Sá, R. M. de, Miranda, C. S. De, & José, N. M. (2016). Preparation and Characterization of Nanowhiskers Cellulose from Fiber Arrowroot (Maranta arundinacea). *Materials Research*, *18*(suppl 2), 225–229.

Sanmuga Priya, E., & Senthamil Selvan, P. (2017). Water hyacinth (Eichhornia crassipes) – An efficient and economic adsorbent for textile effluent treatment – A review. *Arabian Journal of Chemistry*, *10*, S3548–S3558.

Santos, R. M. dos, Flauzino Neto, W. P., Silvério, H. A., Martins, D. F., Dantas, N. O., & Pasquini, D. (2013). Cellulose nanocrystals from pineapple leaf, a new approach for the reuse of this agro-waste. *Industrial Crops and Products*, *50*, 707–714.

Shanmugarajah, B., Loo, P., Mei, I., Chew, L., Yaw, S., & Tan, K. W. (2015). Isolation of NanoCrystalline Cellulose (NCC) from Palm Oil Empty Fruit Bunch (EFB): Preliminary Result on FTIR and DLS Analysis. *Chemical Engineering Transactions*, *45*(March), 1705–1710.

Sindhu, R., Binod, P., Pandey, A., Madhavan, A., Alphonsa, J. A., Vivek, N., … Faraco, V. (2017). Water hyacinth a potential source for value addition: An overview. *Bioresource Technology*, *230*, 152–162.

Soetaredjo, F. ., Ju, Y. ., & Ismadji, S. (2016). Conversion of water hyacinth into biofuel intermediate: combination subcritical water and zeolite based catalyst processes. *The 1st International Workshop Development of Renewable Energy for the Mekong Delta, 14 March 2016*, 64–69.

Stamenković, O. S., Kostić, M. D., Radosavljević, D. B., & Veljković, V. B. (2018). Comparison of Box-Behnken, Face Central Composite and Full Factorial Designs in Optimization of Hempseed Oil Extraction by n-Hexane: a Case Study. *Periodica Polytechnica Chemical Engineering*, *62*(3), 359–367.

Taflick, T., Schwendler, L. A., Rosa, S. M. L., Bica, C. I. D., & Nachtigall, S. M. B. (2017). Cellulose nanocrystals from acacia bark–Influence of solvent extraction. *International Journal of Biological Macromolecules*, *101*, 553–561.

Thambiraj, S., & Ravi Shankaran, D. (2017). Preparation and physicochemical characterization of cellulose nanocrystals from industrial waste cotton. *Applied Surface Science*, *412*, 405–416.

Thi, B. T. N., Thanh, L. H. V, Lan, T. N. P., Thuy, N. T. D., & Ju, Y. (2017). Comparison of Some Pretreatment Methods on Cellulose Recovery from Water

Hyacinth (Eichhornia Crassipe). *Journal of Clean Energy Technologies*, *5*(4), 274–279.

Wang, Z., Yao, Z., Zhou, J., & Zhang, Y. (2017). Reuse of waste cotton cloth for the extraction of cellulose nanocrystals. *Carbohydrate Polymers*, *157*, 945–952.

Wulandari, W. T., Rochliadi, A., & Arcana, I. M. (2016). Nanocellulose prepared by acid hydrolysis of isolated cellulose from sugarcane bagasse. *IOP Conference Series: Materials Science and Engineering*, *107*(1), 12045.

Xie, J., Hse, C.-Y., De Hoop, C. F., Hu, T., Qi, J., & Shupe, T. F. (2016). Isolation and characterization of cellulose nanofibers from bamboo using microwave liquefaction combined with chemical treatment and ultrasonication. *Carbohydrate Polymers*, *151*, 725–734.

Xu, J., Krietemeyer, E. F., Boddu, V. M., Liu, S. X., & Liu, W.-C. (2018). Production and characterization of cellulose nanofibril (CNF) from agricultural waste corn stover. *Carbohydrate Polymers*, *192*(September 2017), 202–207.

Yahya, M., Lee, H. V, Zain, S. K., Hamid, S. B. A., Lefakane, T. E., Ndibewu, P. P., … Huang, N. M. (2015). *Olymers esearch ournal*. *9*(4).

Yandan, C., Qiaomei, W., Biao, H., Mingjie, H., & Xiaolin, A. (2015). Isolation and characteristics of cellulose and nanocellulose from lotus leaf stalk agro-wastes. *BioResources*, *10*(1), 684–696.

Appendices

Appendix A: Results from RSM with design expert

Table A-1. Design summary

StudyType		Initial Design			Design Model		
Response Surface		Box-Behnken			Quadratic		
Factor	Name	Units	Low Actual	High Actual	Low Coded	High Coded	Mean
A	Temper Ature	^{o}C	40.00	60.00	-1.000	1.000	50
B	Time	min	30.00	60.00	-1.000	1.000	45
C	Acid con certration	%	50.00	65.00	-1.000	1.000	57.5
Response Y1	Name Yield	Units %	Analysis Polynomial	Minimum 28.020	Maximum 37.720	Mean 33.014	Std. Dev. 2.993

A-1. Design Matrix Evaluation for Response Surface Quadratic Model

No aliases found for Quadratic Model. Aliases are calculated based on response selection, taking into account missing datapoints, if necessary.

Degrees of Freedom for Evaluation

Model	9
Residuals	5
Lack 0f Fit	3
Pure Error	2
Corr Total	14

A recommendation is a minimum of 3 lack of fit df and 4 df for pure error. This ensures a valid lack of fit test. Fewer df will lead to a test that may not detect lack of fit.

Term	StdErr**	VIF	Ri-Squared	Power at 5 % alpha level for effect of 0.5 Std. Dev.	1 Std. Dev.	2 Std. Dev.
A	0.35	1.00	0.0000	9.0 %	21.1 %	62.3 %
B	0.35	1.00	0.0000	9.0 %	21.1 %	62.3 %
C	0.35	1.00	0.0000	9.0 %	21.1 %	62.3 %
AB	0.50	1.00	0.0000	7.0 %	13.0 %	36.8 %
AC	0.50	1.00	0.0000	7.0 %	13.0 %	36.8 %
BC	0.50	1.00	0.0000	7.0 %	13.0 %	36.8 %
A^2	0.52	1.01	0.0110	12.4 %	34.5 %	86.3 %
B^2	0.52	1.01	0.0110	12.4 %	34.5 %	86.3 %
C^2	0.52	1.01	0.0110	12.4 %	34.5 %	86.3 %

Basis Std. Dev. = 1.0

Measures Derived From the $(X'X)^{-1}$ Matrix

Std	Leverage	Point Type
1	0.7500	IBFact
2	0 .7500	IBFact
3	0.7500	IBFact
4	0.7500	IBFact
5	0.7500	IBFact
6	0.7500	IBFact
7	0.7500	IBFact
8	0.7500	IBFact
9	0.7500	IBFact
10	0.7500	IBFact
11	0.7500	IBFact
12	0.7500	IBFact
13	0.3333	Center
14	0.3333	Center
15	0.3333	Center

Average =0.6667

Appendix B: IR Spectrum Table by Frequency Range

Absorption (cm^{-1})	Appearance	Group	Compound Class
3700-3584	medium, sharp	O-H stretching	Alcohol
3550-3200	strong, broad	O-H stretching	Alcohol
3500	Medium	N-H stretching	primary amine
3400-3300	Medium	N-H stretching	aliphatic primary amine
3350-3310	Medium	N-H stretching	secondary amine
3300-2500	strong, broad	O-H stretching	carboxylic acid
3200-2700	weak, broad	O-H stretching	Alcohol
3000-2800	strong, broad	N-H stretching	amine salt
3333-3267	strong, sharp	C-H stretching	Alkyne
3100-3000	Medium	C-H stretching	Alkene
3000-2840	Medium	C-H stretching	Alkane
2830-2695	Medium	C-H stretching	Aldehyde
2600-2550	Weak	S-H stretching	Thiol
2349	Strong	O=C=O stretching	carbon dioxide
2275-2250	strong, broad	N=C=O stretching	Isocyanate
2260-2222	Weak	CΞN stretching	Nitrile
2260-2190	Weak	CΞC stretching	Alkyne
2175-2140	Strong	S-CΞN stretching	Thiocyanate
2160-2120	Strong	N=N=N stretching	Azide
2150		C=C=O stretching	Ketene
2145-2120	Strong	N=C=N stretching	Carbodiimide
2140-2100	Weak	CΞC stretching	Alkyne
2140-1990	Strong	N=C=S stretching	Isothiocyanate
2000-1900	medium	C=C=C stretching	Allene
2000		C=C=N stretching	Ketenimine
2000-1650	Weak	C-H bending	aromatic compound
1818	Strong	C=O stretching	Anhydride
1815-1785	Strong	C=O stretching	acid halide
1800-1770	Strong	C=O stretching	conjugated acid halide
1775	Strong	C=O stretching	conjugated anhydride
1770-1780	Strong	C=O stretching	vinyl / phenyl ester
1760	Strong	C=O stretching	carboxylic acid
1750-1735	Strong	C=O stretching	Esters
1750-1735	Strong	C=O stretching	δ-lactone
1745	Strong	C=O stretching	Cyclopentanone
1740-1720	Strong	C=O stretching	Aldehyde

1730-1715	Strong	C=O stretching	α, β-unsaturated ester
1725-1705	Strong	C=O stretching	aliphatic ketone
1720-1706	Strong	C=O stretching	carboxylic acid
1710-1680	Strong	C=O stretching	conjugated acid
1710-1685	Strong	C=O stretching	conjugated aldehyde
1690	Strong	C=O stretching	primary amide
1690-1640	medium	C=N stretching	imine / oxime
1685-1666	Strong	C=O stretching	conjugated ketone
1680	Strong	C=O stretching	secondary amide
1680	Strong	C=O stretching	tertiary amide
1650	Strong	C=O stretching	δ-lactam
1678-1668	Weak	C=C stretching	Alkene
1675-1665	Weak	C=C stretching	Alkene
1675-1665	Weak	C=C stretching	Alkene
1662-1626	medium	C=C stretching	Alkene
1658-1648	medium	C=C stretching	Alkene
1650-1600	medium	C=C stretching	conjugated alkene
1650-1580	medium	N-H bending	Amine
1650-1566	medium	C=C stretching	cyclic alkene
1648-1638	Strong	C=C stretching	Alkene
1620-1610	Strong	C=C stretching	α, β-unsaturated ketone
1550-1500	Strong	N-O stretching	nitro compound
1465	medium	C-H bending	Alkane
1450	medium	C-H bending	Alkane
1390-1380	medium	C-H bending	Aldehyde
1385-1380	medium	C-H bending	Alkane
1440-1395	medium	O-H bending	carboxylic acid
1420-1330	medium	O-H bending	Alcohol
1415-1380	Strong	S=O stretching	Sulfate
1410-1380	Strong	S=O stretching	sulfonyl chloride
1400-1000	Strong	C-F stretching	fluoro compound
1390-1310	medium	O-H bending	Phenol
1372-1335	Strong	S=O stretching	Sulfonate
1370-1335	Strong	S=O stretching	Sulphonamide
1350-1342	Strong	S=O stretching	sulfonic acid
1350-1300	Strong	S=O stretching	Sulfone
1342-1266	Strong	C-N stretching	aromatic amine
1310-1250	Strong	C-O stretching	aromatic ester

1275-1200	Strong	C-O stretching	alkyl aryl ether
1250-1020	medium	C-N stretching	Amine
1225-1200	Strong	C-O stretching	vinyl ether
1210-1163	Strong	C-O stretching	Ester
1205-1124	Strong	C-O stretching	tertiary alcohol
1150-1085	Strong	C-O stretching	aliphatic ether
1124-1087	Strong	C-O stretching	secondary alcohol
1085-1050	strong	C-O stretching	primary alcohol
1070-1030	strong	S=O stretching	Sulfoxide
1050-1040	strong, broad	CO-O-CO stretching	Anhydride
995-985	strong	C=C bending	Alkene
980-960	strong	C=C bending	Alkene
895-885	strong	C=C bending	Alkene
850-550	strong	C-Cl stretching	halo compound
840-790	medium	C=C bending	Alkene
730-665	strong	C=C bending	Alkene
690-515	strong	C-Br stretching	halo compound
600-500	strong	C-I stretching	halo compound
880 ± 20	strong	C-H bending	1,2,4-trisubstituted
880 ± 20	strong	C-H bending	1,3-disubstituted
810 ± 20	strong	C-H bending	1,4-disubstituted or
780 ± 20	strong	C-H bending	1,2,3-trisubstituted
755 ± 20	strong	C-H bending	1,2-disubstituted

Appendix C: Some common producers during lab work

Water hyacinth

Size reduction

Extraction

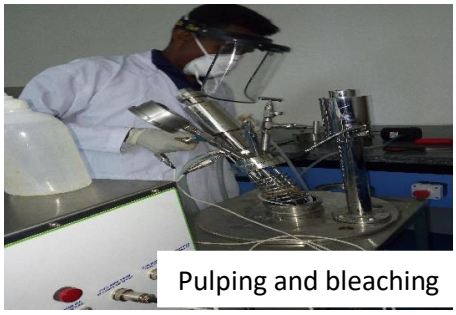

Pulping and bleaching

Acid hydrolysis

Freeze drying